The 4th Joint International Conference on Multibody System Dynamics
May 29 – June 2, 2016, Montréal, Canada

Discrete kinematics of Cosserat rods based on the difference geometry of framed curves

Joachim Linn[1]

[1] *Fraunhofer ITWM, joachim.linn@itwm.fraunhofer.de*

ABSTRACT *The theory of Cosserat rods provides versatile models for the simulation of large spatial deformations of slender flexible structures. As the strain measures of the mechanical theory are given in terms of the differential invariants of Cosserat curves, the kinematics of Cosserat rods are closely related to the differential geometry of framed curves. We utilize ideas from the difference geometry of framed curves in Euclidean space to construct the discrete kinematics of Cosserat rod models on a staggered grid, preserving the essential geometric properties independent of the coarseness of the discretization. On this basis, we also derive a vertex based model variant and discuss its relation to the discrete Cosserat rod kinematics obtained by a geodesic interpolation of the nodal variables in the Lie groups* $\mathbb{E}^3 \times \mathsf{SO}(3)$ *and* $\mathsf{SE}(3)$.

1 Introduction

The theory of *Cosserat rods* [2, 32, 36] provides the proper framework for structural models suitable for physically correct simulations of large deformations of slender flexible objects in space that are primarily governed by a substantial amount of *bending* and *twisting*. Typical examples of such structures from automotive industry are tubes, hoses, single cables, or wiring harnesses collecting many cables within a compound structure (see Fig. 1).

The additional deformation modes of longitudinal *stretching* and transverse *shearing*, which are likewise possible for Cosserat rods, are always neglibly small small in practise, such that they may even be inhibited a priori by imposing internal constraints (as in the case of *inextensible Kirchhoff rods*) without observing a significant impact on the deformed shape of the rod, consistent with Berdichevsky's theoretical results obtained from variational asymptotic analysis [5, 6]. Due to the slenderness of the geometry — i.e.: typical cross section diameters d are small relative to typical lengths L of the considered structures, such that $d/L \ll 1$ holds — the local strains in deformed configurations remain small throughout all steps of a deformation sequence, such that it is possible to use simple linear elastic constitutive relations, which are directly measurable on the structural level, to capture the structural response with sufficient accuracy.

The kinematics of Cosserat rods is closely related to the *differential geometry of framed curves* [9, 10, 15, 20], as the strain measures of a Cosserat rod are given by the differential invariants of a framed curve [2]. We construct the *discrete kinematics* of Cosserat rod models in a way that preserves the essential geometric properties independent of the coarseness of the discretization, utilizing ideas from the *discrete* differential geometry (*DDG*) of framed curves [7, 11, 34, 40]. As our previous work [24, 25] demonstrates, this leads to many favourable properties of discrete Cosserat rod models constructed on this kinematical basis within the variational framework of *(semi)discrete Lagrangian mechanics*. Although the DDG background of our (non–standard) approach to construct discrete geometrically exact rod models based on discrete strain measures obtained via *geometric finite differences* had already been mentioned in an early note [28] and later was at least briefly addressed in the aformentioned articles, it has never been thoroughly explained. With this article[1] we close this gap.

[1] Parts of the discrete kinematical theory for Cosserat rods are presented in slightly modified form in the forthcoming book article [27], together with an extended discussion of industrial applications similar to the ones mentioned in Fig. 1.

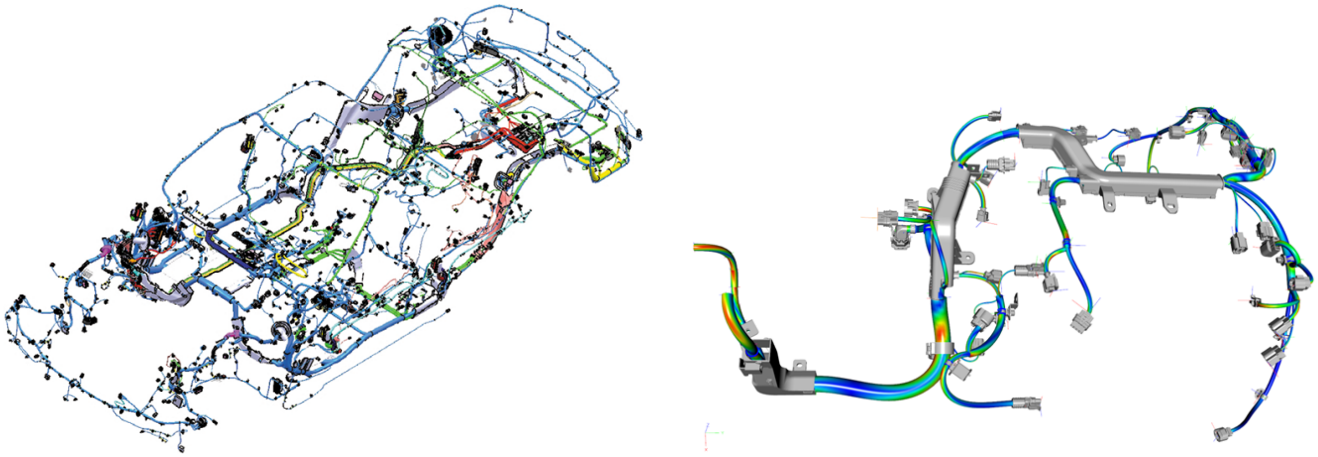

Fig. 1: Overview of the system of cables installed in a car (*left*), and simulation model of a wiring harness in the *IPS Cable Simulation* software (*right*).

In computational mechanics, nonlinear finite element techniques [14, 19, 22] are applied almost exclusively to discretize Cosserat rod models. Geometric aspects as the ones mentioned above are usually disregarded when the shape functions proposed for the interpolation of the configuration variables are introduced. More recent (and less standard) approaches that consider Cosserat rods within the *Lie group* setting [37, 38] are an exception: Here the geometrical properties of Cosserat curves are addressed implicitely by confining interpolated configurations to the group $\mathsf{SE}(3) = \mathbb{E}^3 \rtimes \mathsf{SO}(3)$ of rigid body motions in Euclidean space. Piecewise geodesic interpolation between nodal variables on $\mathsf{SE}(3)$ (considered as a Riemannian manifold) results in an element formulation with *helicoidal shape functions* [13], displaying element-wise constant strains [18]. Similarily, a piecewise geodesic interpolation on the direct product manifold $\mathbb{E}^3 \times \mathsf{SO}(3)$ with rotational d.o.f. represented by unit quaternions yields discrete Cosserat curves consisting of *polygonal centerlines*, augmented by moving frames obtained by *SLERP* interpolation along great circular arcs [35] on the sphere S^3, revealing the geometric background of the interpolation of nodal $\mathsf{SO}(3)$ variables proposed by [19], as shown[2] in [33].

The fact that despite the usage of geodesic shape functions in $\mathbb{E}^3 \times \mathsf{SO}(3)$ *reduced integration* is required to prevent shear locking in the rod model indicates that a sophisticated mathematical reinterpretation of a standard discretization scheme does not necessarily solve known problems, even if geometric aspects within advanced mathematical concepts as Riemannian geometry on manifolds are considered. However, applying the very same approach to the manifold $\mathsf{SE}(3)$ does indeed yield locking free Cosserat rod elements, as additional aspects of the geometric properties of the theory are accounted for: Due to the Lie group structure of the configuration manifold, the differential invariants (respectively: strain measures) appear in a canonical way as components of a *left–invariant vector field* within the basic kinematic equations [38]. A discrete model constructed via a geodesic interpolation of element-wise constant invariants on $\mathsf{SE}(3)$ will likewise possess this property and behave qualitatively correct even for coarse discretisations.

Moreover, a closer look into the constructive proof of the *principal theorem of the differential geometry of framed curves* reveals that the core arguments brought forward in the course of the proof may be reformulated equivalently within the treatment of Cosserat curves in the *Lie group* setting of the configuration manifold $\mathsf{SE}(3)$. As readers familiar with the differential geometry of framed curves in Euclidean space will know, this mathematical theory is usually formulated, and all essential results are derived, without *any* necessitiy of reference to Lie group theory, which is typically not available at the undergraduate level where this material is usually presented within the framework of advanced calculus. Nevertheless, the choice of the differential invariants within the traditional framework appears to be somewhat *ad hoc*, motivated by analytical arguments, e.g. for utilizing derivatives of a space curve w.r.t. its parameter to lowest possible (i.e.: up to third) order, rather than by geometric aspects.

[2]Note that although in [33] the author explicitely aims at the construction of geodesic finite elements for Cosserat rods considered as curves in the *semidirect* product manifold $\mathsf{SE}(3)$, the shape functions obtained in this work are in fact piecewise geodesic curves in the *direct* product manifold $\mathbb{E}^3 \times \mathsf{SO}(3)$, with SLERP interpolation for the rotational quaternions [35] used for local parametrization.

As a consequence, the fact that there are better choices to frame a space curve [8] than Frenet's trihedron is still rarely known, although it dates back to G. Darboux's work and has been presented in the classical mathematics literature of the late 19^{th} and early 20^{th} century (see e.g. [9]). As suggested by the authors of [37, 38], the proper choice of invariants for framed space curves emerges in a canonical way within the Lie group setting, which removes the aforementioned ad hoc arguments present in the classical treatment, although this is achieved at the prize of a substantial increase in technical complication of the required mathematical tools.

Different from a nonlinear FE approach aiming at weak solutions of the mechanical equilibrium equations [41], we consider Cosserat rod models within the variational framework of *Lagrangian mechanics* in terms of the kinetic and elastic energy of the rod [24, 25, 28], as outlined in appendix B. In particular, as the elastic energy density of a rod is given as a quadratic form in the strain measures, we obtain the *discrete* elastic energy by an approach which we denote as *geometric finite differences*, which provides a consistent discretization of the strain measures that preserves their essential geometric properties, in combination with simple quadrature rules to approximate the terms of the integrated energy density (see appendix C). Due to the geometric discretization of the strains, discrete rod models constructed according to our discrete Lagrangian mechanics approach behave qualitatively correct even for very coarse discretizations, provide fast computational performance at good accuracy, as determined by the order of the chosen discretization scheme.

In our article, we introduce the basic ideas of our geometry based discretization approach for flexible slender structures as sketched above. The mathematical backbone of our construction of discrete Cosserat rod models is provided by the difference geometry of framed curves in the spirit of Sauer's approach [34] to discrete Frenet curve theory. We present an extension of Sauer's ideas to construct the basic constituents of the discrete geometry of Cosserat curves in Euclidian space, including proper definitions of discrete curvatures, discrete generalized Frenet equations with geometrically exact solutions in terms of finite rotations, all summarized in the formulation of a *principal theorem of discrete Cosserat curve theory*. On this basis, the construction of discrete Cosserat rod models formulated in terms of discrete elastic energy functions, defined as quadratic forms of the invariants of discrete Cosserat curves, can be obtained in a straightforward manner (see appendix C). We also derive a *vertex based* model variant and discuss its relation to the discrete Cosserat rod kinematics obtained by a geodesic interpolation of the nodal variables in the Lie groups $\mathbb{E}^3 \times \mathsf{SO}(3)$ and $\mathsf{SE}(3)$.

2 Cosserat curves as kinematical skeletons of slender material bodies

Following Antman [2], the mathematical notion of a *material body* is that of a topological manifold $\mathscr{X}$ that is homeomorphically mapped to *regions in Euclidean point space*. This means that the elements $x \in \mathscr{X}$ (denoted as *abstract material particles*) are mapped to points $p(x) \in \mathscr{E}^3$ in Euclidean space, such that the mapping $x \mapsto p = \chi(x)$ is invertible and (at least) continuous. Then the set $\mathscr{B} := \{p \in \mathscr{E}^3 | p = \chi(x), x \in \mathscr{X}\} = \chi(\mathscr{X})$ is a *configuration* of $\mathscr{X}$ in Euclidean point space $\mathscr{E}^3$ (see appendix A).

A *Cosserat rod* is a material body of slender shape. Its configuration $\mathscr{B}_C$ can be well represented by a *Cosserat curve*, i.e.: a geometric curve $\mathscr{C} \subset \mathscr{B}_C \subset \mathscr{E}^3$, augmented by a triple $\{\mathbf{a}^{(1)}(p), \mathbf{a}^{(2)}(p), \mathbf{a}^{(3)}(p)\}$ of *orthonormal directors* located in the points $p \in \mathscr{C}$. For fixed $p \in \mathscr{C}$ the two directors $\mathbf{a}^{(1,2)}(p)$ span an affine plane in $\mathbb{E}^3$ that is uniquely determined by the curve point p and the normal vector $\mathbf{a}^{(3)}(p) = \mathbf{a}^{(1)}(p) \times \mathbf{a}^{(2)}(p)$ and contains all material points of the local cross section area $\mathscr{A}(p)$ of the rod located at p. The latter can be parametrized by a pair of cartesian coordinates $(\xi_1, \xi_2) \in A_p \subset \mathbb{R}^2$, such that the material points $x \in \mathscr{B}_C \subset \mathscr{E}^3$ of a Cosserat rod configuration $\mathscr{B}_C$ are given by the relation $x = p + \xi_\alpha \mathbf{a}^{(\alpha)}(p)$. As the curve $\mathscr{C}$ is assumed to be regular, it can be parametrized by arc length as $s \mapsto p(s)$, such that the whole configuration $\mathscr{B}_C \in \mathscr{E}^3$ is given as a parametrized region in $\mathscr{E}^3$, with points given by: $x(\xi_1, \xi_2, s) = p(s) + \xi_\alpha \mathbf{a}^{(\alpha)}(p(s))$.

In this sense, Cosserat curves provide *kinematical skeletons* for a curvilinear parametrization of configurations of material bodies of slender shape (i.e.: long and thin, with cross section diameters considerably smaller than longitudinal dimensions). Therefore, the *strain measures* of such bodies are determined by the invariants of a Cosserat curve, and their elastic energy is likewise given as a function of these invariants (see appendix B).

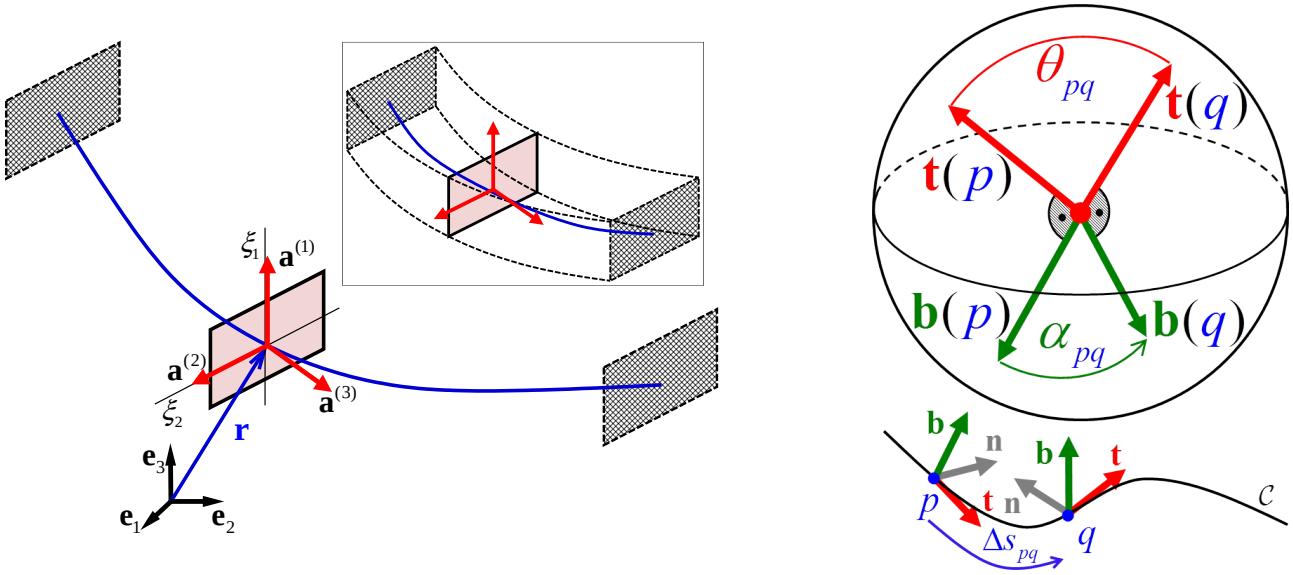

Fig. 2: *Left:* Centerline curve $\mathbf{r}(s)$ and attached moving frame $\mathsf{R}(s) = \mathbf{a}^{(k)}(s) \otimes \mathbf{e}_k$ of a *Cosserat curve*, describing the geometry of the configurations of a prismatic rod in Euclidian space. The volumetric geometry is generated by sliding the cross section spanned by the frame directors $\{\mathbf{a}^{(1)}, \mathbf{a}^{(2)}\}$ along the centerline. The position vectors of the material points in the rod volume are parametrized by: $\mathbf{x} = \mathbf{r}(s) + \xi_\alpha \, \mathbf{a}^{(\alpha)}(s)$. *Right:* For points $p \in \mathscr{C}$ of a smooth geometric curve the *tangent map* $p \mapsto \mathbf{t}(p)$ induces a curve on the unit sphere $S^2 \subset \mathbb{E}^3$. For pairs $(p,q) \in \mathscr{C}$ located at distance Δs_{pq} the shortest path on S^2 connecting their tangent vectors $\mathbf{t}(p)$ and $\mathbf{t}(q)$ is a circular arc of length θ_{pq}. In the limit $\Delta s_{pq} \to 0$ the ratio $\theta_{pq}/\Delta s_{pq}$ converges to the *Frenet curvature* $\kappa(p)$. The *binormal map* $p \mapsto \mathbf{b}(p)$ is well defined on curve segments of positive curvature. The *geometric torsion* $\tau(p)$ is obtained from the ratio $\alpha_{pq}/\Delta s_{pq}$ of the signed length α_{pq} of the circular arc connecting the binormals $\mathbf{b}(p)$ and $\mathbf{b}(q)$ to the arc length distance of the curve points in the same limit.

Basic differential geometry of framed parameter curves As outlined above, the slender geometry of the parts considered provides the possibility to reduce the continuum model analytically to an object which is well known (and likewise well understood) in classical differential geometry, namely: a *framed parameter curve* (or parametrized *Cosserat curve*) consisting of [2, 16]

- a space curve $\mathbf{r}(s)$ corresponding to the *centerline* of the rod, and
- a *moving frame* $\mathsf{R}(s) = \mathbf{a}^{(j)}(s) \otimes \mathbf{e}_j$ of orthonormal directors,

where the pair $\{\mathbf{a}^{(1)}(s), \mathbf{a}^{(2)}(s)\}$ spans the local cross section of the rod at the position $\mathbf{r}(s)$, such that the unit length *cross section normal* vector is given by $\mathbf{a}^{(3)}(s) = \mathbf{a}^{(1)}(s) \times \mathbf{a}^{(2)}(s)$, as sketched in Fig. 2.

As $\mathbf{r}(s) \in \mathbb{E}^3$ and $\mathsf{R}(s) \in \mathsf{SO}(3)$, a Cosserat curve is a parameter curve in the manifold $\mathbb{E}^3 \times \mathsf{SO}(3)$ of rigid body configurations[3] in Euclidian space. The curve parameter s is usually assumed to correspond to the *arc length* of $\mathbf{r}(s)$, such that the tangent vector $\mathbf{t}(s) = \mathbf{r}'(s)$ has unit length. The frame $\mathsf{R}(s)$ is called *adapted* to the curve if $\mathbf{a}^{(3)}(s) = \mathbf{t}(s)$ holds. While in the setting of classical differential geometry of framed curves mainly adapted frames are considered, *non-adapted* frames are of primary interest in the kinematical theory of *geometrically exact rods*, where adapted frames merely occur as a special case, recoverable from a kinematically more general Cosserat curve by the *Euler–Bernoulli* constraint $\mathbf{r}'(s) = \mathbf{a}^{(3)}(s)$, enforcing cross sections to remain orthogonal to the tangent vector of an inextensible centerline curve.

Frenet curves and ribbons The most well known adapted frame in elementary differential geometry of space curves is the *Frenet* frame $(\mathbf{a}^{(1)}, \mathbf{a}^{(2)}, \mathbf{a}^{(3)}) = (\mathbf{n}, \mathbf{b}, \mathbf{t})$, consisting of the *principal normal* and *binormal* vectors defined as $\mathbf{n}(s) := \mathbf{t}'(s)/\kappa(s)$ and $\mathbf{b}(s) := \mathbf{t}(s) \times \mathbf{n}(s)$ on intervals of non-zero Frenet curvature $\kappa(s) := \|\mathbf{t}'(s)\|$ (see Fig. 2). More general, one may consider parameter curves on oriented surface patches, with the (likewise adapted) *Darboux frame* of the curve defined by the curve tangent $\mathbf{t}$ and the unit length normal vector field $\mathbf{N}$ of the surface at

[3] One should distinguish the configuration manifold $\mathbb{E}^3 \times \mathsf{SO}(3)$ of rigid bodies in Euclidean space from the transformation group $\mathsf{SE}(3)$ of rigid body motions, see Ch. 6 in [3].

the curve points. This leads to the notion of a *ribbon* (or *surface strip*), defined as a surface patch of infinitesimally small width around a curve $\mathbf{r}(s)$, oriented by a unit vector $\mathbf{N}(s)$ orthogonal to the tangent vector $\mathbf{t}(s)$ of the curve, with an adapted frame given by: $(\mathbf{a}^{(1)},\mathbf{a}^{(2)},\mathbf{a}^{(3)}) = (\mathbf{N},\mathbf{t}\times\mathbf{N},\mathbf{t})$.

From a slightly different point of view, one may consider an arbitrary frame field $\mathsf{R}(s)$, given as a parameter curve in $\mathsf{SO}(3)$, and recover its corresponding space curve by integration: $\mathbf{r}'(s) = \mathbf{a}^{(3)}(s) \;\Leftrightarrow\; \mathbf{r}(s) = \mathbf{r}_0 + \int_0^s \mathbf{a}^{(3)}(\zeta)\,d\zeta$. The evolution of the adapted frame of a ribbon along its curve is determined by the generalized Frenet equations $\partial_s \mathbf{a}^{(k)}(s) = \boldsymbol{\kappa}(s)\times\mathbf{a}^{(k)}(s)$. The curvatures $\varkappa^{(k)}(s)$ are defined as the components of the the *Darboux vector* $\boldsymbol{\kappa} = \varkappa^{(j)}\,\mathbf{a}^{(j)} = \frac{1}{2}\partial_s\mathbf{a}^{(j)}\times\mathbf{a}^{(j)} = \kappa\,\mathbf{b} + \varkappa^{(3)}\,\mathbf{t}$ w.r.t. the directors of the moving frame. If they are given as continuous functions of arc length, they provide a complete set of differential invariants that determine the geometry of a ribbon up to a global rigid body motion.

Cosserat curves and quaternion frames Cosserat curves may be considered as natural generalizations of ribbons by omitting the requirement of an adaption of the frame to the curve. In the context of the kinematics of geometrically exact rods one proceeds even one step further by considering regular curves that are not necessarily parametrized by arc length: If one resolves the tangent vector $\mathbf{r}'(\zeta)$ w.r.t. the directors of the moving frame $\mathsf{R}(\zeta) = \mathbf{a}^{(k)}(\zeta)\otimes\mathbf{e}_k$, then the components $\Gamma^{(k)}(\zeta) := \langle\mathbf{a}^{(k)}(\zeta),\mathbf{r}'(\zeta)\rangle$ of the tangent vector, together with the curvatures $K^{(k)}(\zeta)$, which are implicitely given by the frame equations $\partial_\zeta\mathbf{a}^{(k)} = \boldsymbol{\kappa}\times\mathbf{a}^{(k)}$ and associated Darboux vector $\boldsymbol{\kappa}(\zeta) = K^{(j)}(\zeta)\,\mathbf{a}^{(j)}(\zeta)$, provide a complete set of differential invariants that determine a Cosserat curve up to a global rigid body motion.

The proof of this statement, which constitutes the *principal theorem* of the differential geometry of Cosserat curves, may be obtained by a straightforward adaption of the corresponding one for ribbons (see [2]): For given curvature functions $K^{(j)}(\zeta)$, the frame equations become a system of linear ODEs for the frame directors that can be integrated for an arbitrary initial value $\mathsf{R}_0\in\mathsf{SO}(3)$ according to the theory of ordinary differential equations. Due to the special algebraic structure of the frame equations, the scalar products of the frame directors are conserved (i.e.: $\langle\mathbf{a}^{(i)}(\zeta),\mathbf{a}^{(j)}(\zeta)\rangle = \delta_{ij}$), such that the solution $\mathsf{R}(\zeta) = \mathbf{a}^{(j)}(\zeta)\otimes\mathbf{e}_j$ always remains in $\mathsf{SO}(3)$. For given $\boldsymbol{\Gamma}(\zeta) := \Gamma^{(j)}(\zeta)\,\mathbf{e}_j$ and known $\mathsf{R}(\zeta)$, the tangent vector $\mathbf{r}'(\zeta) = \Gamma^{(j)}(\zeta)\,\mathbf{a}^{(j)}(\zeta) = \mathsf{R}(\zeta)\cdot\boldsymbol{\Gamma}(\zeta)$ can then be considered as a known function that can subsequently be integrated, which finally yields the space curve $\mathbf{r}(\zeta) = \mathbf{r}_0 + \int_0^\zeta \mathsf{R}(\xi)\cdot\boldsymbol{\Gamma}(\xi)\,d\xi$ for an arbitrarily chosen initial value $\mathbf{r}_0$.

Note that as $\|\mathbf{r}'(\zeta)\| = \|\boldsymbol{\Gamma}(\zeta)\|$ holds, the differential of arc length is given by $ds = \|\boldsymbol{\Gamma}(\zeta)\|\,d\zeta$, such that one may always reparametrize a regular Cosserat curve by its arc length function $s(\zeta)$, with a corresponding rescaling of the curvatures according to: $\varkappa^{(k)}(s) = K^{(k)}(\zeta)/\|\boldsymbol{\Gamma}(\zeta)\|$. For curves parametrized by arc length $\Gamma^{(k)}(s) = \langle\mathbf{a}^{(k)}(s),\mathbf{t}(s)\rangle$ are the direction cosines of the tangent vector w.r.t. the local frame axes. Ribbons consisting of regular curves parametrized by arc length with adapted frames correspond to the special case of constant $\boldsymbol{\Gamma}_0 = (0,0,1)^T \equiv \mathbf{e}_3$. Frenet curves may in turn be considered as special cases of ribbons, with their Darboux vector given by $\boldsymbol{\kappa} = \kappa\,\mathbf{b} + \tau\,\mathbf{t}$.

The formulation of Cosserat rod models as presented in [25] is based on *quaternionic Cosserat curves*, where the moving frame $\mathsf{R}(s)$ is represented equivalently by a moving unimodular (*rotational*) quaternion field $\hat{\mathsf{q}}(s)$, characterized by the identity $\mathsf{R}(s)\cdot\mathbf{v} = \hat{\mathsf{q}}(s)\circ\mathbf{v}\circ\hat{\mathsf{q}}^*(s)$ holding for arbitrary vectors $\mathbf{v}\in\mathbb{E}^3\simeq\Im\mathbb{H}$. The generalized Frenet equations can be written equivalently in terms of a derivative equation $\mathsf{R}'(s) = \mathsf{R}(s)\cdot\tilde{\mathsf{K}}(s)$ for the moving frame, using the skew matrix $\tilde{\mathsf{K}}\in\mathfrak{so}(3)$ associated to the *material Darboux vector* $\mathbf{K}(s) = K^{(j)}(s)\,\mathbf{e}_j = \mathsf{R}^T(s)\cdot\boldsymbol{\kappa}(s)$.

The derivative equation for the equivalent quaternion frame is given by $\hat{\mathsf{q}}'(s) = \frac{1}{2}\boldsymbol{\kappa}(s)\circ\hat{\mathsf{q}}(s) = \frac{1}{2}\hat{\mathsf{q}}(s)\circ\mathbf{K}(s)$. As $\Re(\mathbf{K}) = 0 = \Re(\boldsymbol{\kappa})$, any solution of this ODE has constant modulus. In particular $|\hat{\mathsf{q}}(s)|\equiv 1$ holds for any solution of the frame equation starting from an initial value $\hat{\mathsf{q}}_0\in S^3$. The recovery formula for the centerline by integration in terms of a solution $\hat{\mathsf{q}}(s)$ of the quaternionic frame equation — determined by the given curvature vector $\mathbf{K}(s)$ and initial value $\hat{\mathsf{q}}_0$ — and given $\boldsymbol{\Gamma}(s)$ may then be reformulated in terms of quaternionic quantities as: $\mathbf{r}(s) = \mathbf{r}_0 + \int_0^s \hat{\mathsf{q}}(\zeta)\circ\boldsymbol{\Gamma}(\zeta)\circ\hat{\mathsf{q}}^*(\zeta)\,d\zeta$. This implies an equivalent formulation of the principal theorem for quaternionic Cosserat curves, which are likewise determined by given functions $\mathbf{K}(s)$ and $\boldsymbol{\Gamma}(s)$ up to a global rigid body motion.

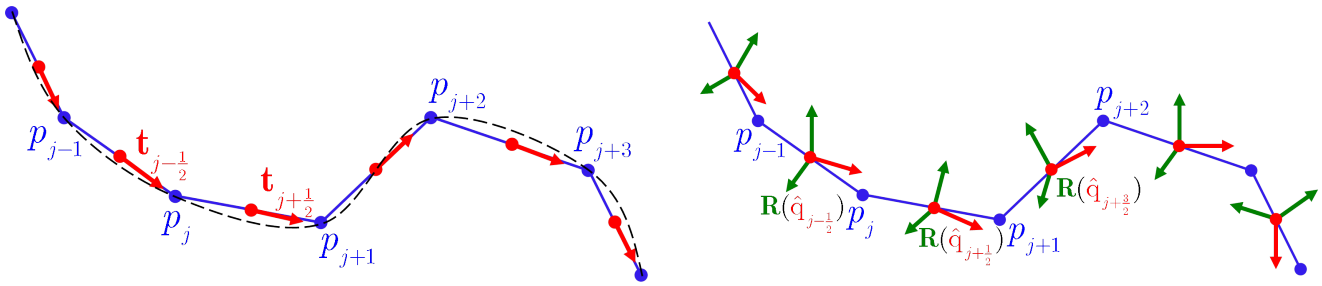

Fig. 3: *Left:* Polygonal arc approximating a smooth regular geometric curve $\mathscr{C}$: The vertices $p_j \in \mathscr{C}$ define the edges $[p_{j-1}, p_j]$ of length $\ell_{j-1/2} > 0$, with tangent vectors $\mathbf{t}_{j-1/2} = (p_j - p_{j-1})/\ell_{j-1/2}$ of unit length located at edge centers $\bar{p}_{j-1/2}$. *Right:* Polygonal arc and edge based quaternionic frames $\hat{\mathfrak{q}}_{j-1/2} \equiv \mathsf{R}_{j-1/2} = \mathfrak{E}(\hat{\mathfrak{a}}_{j-1/2})$ of a *discrete Cosserat curve*.

3 Discrete quaternionic Cosserat curves

In this section we construct the *discrete kinematics* of quaternionic Cosserat rod models, utilizing ideas from the *difference geometry of framed curves* [34], such that essential geometric properties are preserved independent of the coarseness of the discretization.

Discrete regular geometric curves We define a *discrete regular geometric curve* as a mapping $\mathbb{Z} \ni j \mapsto p_j \in \mathscr{E}^3$ of integer indices to points in Euclidean space, where $p_j \neq p_{j-1}$ holds for all vertex pairs (p_{j-1}, p_j), such that unit length *tangent vectors* $\mathbf{t}_{j-1/2} := (p_j - p_{j-1})/\ell_{j-1/2}$ are well defined on all edges (see Fig. 3 on the left). If the vertices $p_j = p(s_j)$ are located on a smooth regular geometric curve $\mathscr{C}$, with arc length parametrization $[0, L] \ni s \mapsto p(s) \in \mathscr{C}$ of its points, the edge centered tangent vectors $\mathbf{t}_{j-1/2}$ approximate tangent vectors $\mathbf{t}(p_{j-1/2})$ of $\mathscr{C}$ in points $p_{j-1/2} := p(s_{j-1/2})$ located at half arc length distance $\frac{1}{2}(s_{j-1} + s_j) =: s_{j-1/2}$ between adjacent vertices (p_{j-1}, p_j) with 2^{nd} order accuracy. Likewise, the *edge centers* $\bar{p}_{j-1/2}$ approximate the corresponding curve points $p_{j-1/2}$ with the same accuracy. *Discrete arc length* parameters ς_j are defined by the sum $\varsigma_j := \sum_{i=1}^{j} \ell_{i-1/2}$ of edge lengths, such that $\varsigma_j - \varsigma_{j-1} =: \Delta\varsigma_{j-1/2} = \ell_{j-1/2}$ and $\Delta\varsigma_j := \frac{1}{2}(\ell_{j-1/2} + \ell_{j+1/2}) = \varsigma_{j+1/2} - \varsigma_{j-1/2}$ with $\varsigma_{j\pm1/2} := \frac{1}{2}(\varsigma_j + \varsigma_{j\pm1})$ measure the distances of adjacent vertices and edge centers in discrete arc length.

In differential geometry, the approximation of a smooth, at least continuous space curve by a polygonal arc is the canonical starting point to introduce the geometric notion of *arc length* on the discrete level. For locally Lipschitz continuous curves, the discrete approximation converges to the limit of a continuous arc length, defined as the least upper bound of the discrete lengths of approximiating polygonal arcs. Such curves are called *rectifiable*, and their arc length is independent of their state of curvature. The definition of *discrete arc length* given above captures this property in the discrete setting by construction. Higher order interpolation approaches, e.g. by splines, fail to do so. If a curve is differentiable and possesses a non-vanishing tangent in all of its points, it is called *regular*. Our definition of *discrete regularity* given above captures this property on the discrete level as well.

Discrete Frenet curves On this basis, one can proceed to construct a discrete version of Frenet curve theory, along the guidelines briefly discussed in the caption annotating the schematic picture shown in Fig. 2 on the right. The *discrete Frenet curvature* can be defined in terms of the vertex angle θ_j enclosed by edge tangent vectors $\mathbf{t}_{j\pm1/2}$, separated by discrete arc length distance $\Delta\varsigma_j$, as $\kappa_j := \theta_j/\Delta\varsigma_j$ (see Fig. 4 on the left). *Discrete binormal vectors* $\mathbf{b}_j \sim \mathbf{t}_{j-1/2} \times \mathbf{t}_{j+1/2}$ (normalized to unit length) are well defined in all vertices between non-aligned edges, such that the *discrete geometric torsion* $\tau_{j+1/2} := \alpha_{j+1/2}/\ell_{j+1/2}$ can be defined in terms of the angle enclosed by adjacent discrete binormals $\mathbf{b}_j$ and $\mathbf{b}_{j+1}$ separated by discrete arc length distance $\ell_{j+1/2} = \varsigma_{j+1} - \varsigma_j$, as depicted in the middle of Fig. 4. Using these definitions, one can show that the sets $\{\mathbf{t}_{j-1/2}\}_{j=1,\dots,n}$ and $\{\mathbf{b}_j\}_{j=1,\dots,n-1}$ of edge tangent and vertex binormal vectors exactly solve the coupled system of discrete Frenet equations

$$\mathbf{t}_{j+1/2} - \mathbf{t}_{j-1/2} = 2\tan(\theta_j/2)\,\mathbf{b}_j \times \frac{1}{2}(\mathbf{t}_{j+1/2} + \mathbf{t}_{j-1/2})\,, \quad \mathbf{b}_{j+1} - \mathbf{b}_j = -2\tan(\alpha_{j+1/2}/2)\,\frac{1}{2}(\mathbf{b}_j + \mathbf{b}_{j+1}) \times \mathbf{t}_{j+1/2}\,,$$

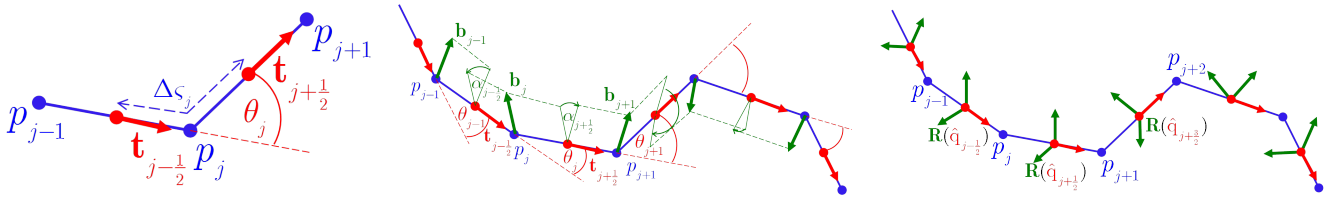

Fig. 4: *Left:* For triples $(p_j, p_{j\pm1})$ of vertices on a discrete regular geometric curve, the *bending angle* θ_j at the intermediate vertex p_j is defined as the non-negative angle enclosed by the pair $\mathbf{t}_{j\pm1/2}$ of adjacent edge tangent vectors and equals the length of the circular arc connecting $\mathbf{t}_{j\pm1/2}$ on S^2. *Middle:* Polygonal arc approximating a Frénet curve: Vertex based bending angles θ_j are defined by pairs $\mathbf{t}_{j\pm1/2}$ of unit length edge tangent vectors, given by triples $(p_j, p_{j\pm1})$ of consecutive vertices. Edge based torsion angles $\alpha_{j+1/2}$ connect pairs $(\mathbf{b}_j, \mathbf{b}_{j+1})$ of vertex binormals by a rotation about the $\mathbf{t}_{j+1/2}$ axis. *Right:* Polygonal arc and edge based frames $\hat{\mathsf{q}}_{j-1/2} \equiv \mathsf{R}_{j-1/2} = \mathfrak{E}(\hat{\mathsf{q}}_{j-1/2})$ of a *discrete ribbon*, which is a special case of a discrete Cosserat curve with *adapted frames*, i.e.: $\mathbf{a}^{(3)}_{j-1/2} = \mathbf{t}_{j-1/2}$.

which is a finite difference discretization of the corresponding continuous equations on a staggered grid. We do not go into further details of discrete Frenet curve theory here, which is discussed in detail in Sauer's book [34]. One may extend the discrete Frenet curve theory by considering egde based *adapted* frames, which leads to the definition of *discrete ribbons* (see Fig. 4 on the right), which have been treated in the articles [11] and [7].

Discrete quaternionic Cosserat curves and their invariants Motivated by the brief discussion of discrete Frenet curves, we define a *discrete Cosserat curve* as a discrete regular geometric curve, augmented by a set $\{\mathsf{R}_{j-1/2}\}_{j=1,\dots,N}$ of *orthonormal frames* $\mathsf{R}_{j-1/2} = \mathbf{a}^{(k)}_{j-1/2} \otimes \mathbf{e}_k \in \mathsf{SO}(3)$ located *at edge centers* $\bar{p}_{j-1/2}$, as sketched in Fig. 3 on the right. The frames are represented by *rotational quaternions* as $\mathsf{R}_{j-1/2} = \mathfrak{E}(\hat{\mathsf{q}}_{j-1/2})$ in terms of the *Euler map* $\mathfrak{E} : S^3 \to \mathsf{SO}(3)$ defined via its operation $\mathfrak{E}(\hat{\mathsf{q}}) \cdot \mathbf{v} = \hat{\mathsf{q}} \circ \mathbf{v} \circ \hat{\mathsf{q}}^*$ on vectors, such that the frame directors are given by: $\mathbf{a}^{(k)}_{j-1/2} = \mathsf{R}_{j-1/2} \cdot \mathbf{e}_k = \hat{\mathsf{q}}_{j-1/2} \circ \mathbf{e}_k \circ \hat{\mathsf{q}}^*_{j-1/2}$.

In the continuum theory the differential invariants that determine the geometry of a quaternionic Cosserat curve uniquely up to a global rigid body motion are: the material curvature vector $\mathbf{K}$ implicitely given by the frame equation $\mathrm{d}\hat{\mathsf{q}}_p = \frac{1}{2}\hat{\mathsf{q}} \circ \mathbf{K}$, and the material tangent vector $\mathbf{\Gamma} = \hat{\mathsf{q}}^* \circ \mathbf{t} \circ \hat{\mathsf{q}}$ obtained by rotating the spatial tangent vector $\mathbf{t}(p) = \mathrm{d}p(p)$ back to the local frame $\hat{\mathsf{q}}(p)$. In the discrete setting, corresponding invariants of a discrete Cosserat curve can be obtained analogously: The *discrete material tangent vectors* $\mathbf{\Gamma}_{j-1/2} := \hat{\mathsf{q}}^*_{j-1/2} \circ \mathbf{t}_{j-1/2} \circ \hat{\mathsf{q}}_{j-1/2}$ result from a back rotation of edge tangent vectors, and the *discrete material curvature vectors* $\mathbf{K}_j := (\vartheta_j/\Delta\varsigma_j)\hat{\mathbf{U}}_j = 2\log(\hat{\mathsf{W}}_j)/\Delta\varsigma_j$ can be extracted from the *material difference rotations*

$$\hat{\mathsf{q}}^*_{j-1/2} \circ \hat{\mathsf{q}}_{j+1/2} \;=:\; \hat{\mathsf{W}}_j \;=\; \cos(\vartheta_j/2) + \sin(\vartheta_j/2)\,\hat{\mathbf{U}}_j \;=\; \exp(\vartheta_j/2\,\hat{\mathbf{U}}_j) \tag{1}$$

that connect adjacent frames $\hat{\mathsf{q}}_{j\pm1/2}$. The corresponding spatial difference rotations are implicitely defined by $\hat{\mathsf{q}}_{j+1/2} = \hat{\mathsf{w}}_j \circ \hat{\mathsf{q}}_{j-1/2}$ and explicitely given by:

$$\hat{\mathsf{q}}_{j+1/2} \circ \hat{\mathsf{q}}^*_{j-1/2} \;=:\; \hat{\mathsf{w}}_j \;=\; \cos(\vartheta_j/2) + \sin(\vartheta_j/2)\,\hat{\mathbf{u}}_j \;=\; \exp(\vartheta_j/2\,\hat{\mathbf{u}}_j)\;,$$

with $\hat{\mathsf{W}}_j = \hat{\mathsf{q}}^*_{j\pm1/2} \circ \hat{\mathsf{w}}_j \circ \hat{\mathsf{q}}_{j\pm1/2}$, and $\hat{\mathbf{u}}_j = \hat{\mathsf{q}}_{j\pm1/2} \circ \hat{\mathbf{U}}_j \circ \hat{\mathsf{q}}^*_{j\pm1/2}$.

Discrete derivative equations for quaternion frames In this paragraph we briefly show that the iteration procedure $\hat{\mathsf{q}}_{j-1/2} \mapsto \hat{\mathsf{q}}_{j+1/2} = \hat{\mathsf{q}}_{j-1/2} \circ \exp(\Delta\varsigma_j/2\,\mathbf{K}_j)$ implied by (1) yields the *exact general solution* of the finite difference equations

$$2\,(\hat{\mathsf{q}}_{j+1/2} - \hat{\mathsf{q}}_{j-1/2}) \;=\; \frac{1}{2}(\hat{\mathsf{q}}_{j-1/2} + \hat{\mathsf{q}}_{j+1/2}) \circ \left[4\tan\left(\frac{\vartheta_j}{4}\right)\hat{\mathbf{U}}_j\right] \tag{2}$$

for the quaternion frames of a discrete Cosserat curve, which is centered at $p = p_j$ and, after division by $\Delta\varsigma_j$, converges to its continuum counterpart $2\mathrm{d}\hat{\mathsf{q}}_{p_j} = \hat{\mathsf{q}}(p_j) \circ \mathbf{K}(p_j)$ in the limit $\Delta\varsigma_j \to 0$.

The desired discretisation can be obtained from the quaternionic Cayley transform[4] and its inverse

$$\mathbf{q} \mapsto \hat{\mathsf{p}} \,=\, \mathrm{cay}(\mathbf{q}) \,=\, \frac{1+\mathbf{q}}{1-\mathbf{q}}\;,\;\; \hat{\mathsf{p}} \mapsto \mathbf{q} = \mathrm{cay}^{-1}(\hat{\mathsf{p}}) \,=\, \frac{\hat{\mathsf{p}}-1}{\hat{\mathsf{p}}+1}\;,$$

mapping vectors to rotational quaternions and vice versa. For $\hat{\mathsf{p}} = \cos(\alpha) + \sin(\alpha)\,\hat{\mathbf{e}} = \exp(\alpha\,\hat{\mathbf{e}})$ one obtains $\mathbf{q} = \mathrm{cay}^{-1}(\hat{\mathsf{p}}) = \tan(\alpha/2)\,\hat{\mathbf{e}}$, such that $\exp(\alpha\,\hat{\mathbf{e}}) = \mathrm{cay}(\tan(\alpha/2)\,\hat{\mathbf{e}})$ holds. Applied to the rotation $\hat{\mathsf{W}}_j = \exp(\vartheta_j/2\,\hat{\mathbf{U}}_j)$ connecting adjacent quaternion frames via $\hat{\mathsf{q}}_{j+1/2} = \hat{\mathsf{q}}_{j-1/2} \circ \hat{\mathsf{W}}_j$, the difference equations (2) emerge after some elementary algebraic rearrangements. Dividing both sides of (2) by $\Delta\varsigma_j$, the desired result is finally obtained in the limit $\Delta\varsigma_j \to 0$, if the limits $\lim_{\Delta\varsigma_j\to 0}\mathbf{K}_j = \mathbf{K}(p_j) = \lim_{\Delta\varsigma_j\to 0}\frac{4}{\Delta\varsigma_j}\tan\left(\frac{\vartheta_j}{4}\right)\hat{\mathbf{U}}_j$, $\mathrm{d}\hat{\mathsf{q}}_{p_j} = \lim_{\Delta\varsigma_j\to 0}(\hat{\mathsf{q}}_{j+1/2} - \hat{\mathsf{q}}_{j-1/2})/\Delta\varsigma_j$ and $\hat{\mathsf{q}}(p_j) = \lim_{\Delta\varsigma_j\to 0}\frac{1}{2}(\hat{\mathsf{q}}_{j-1/2} + \hat{\mathsf{q}}_{j+1/2})$ are taken into account. The corresponding discretisation

$$\hat{\mathsf{q}}_{j+1/2} - \hat{\mathsf{q}}_{j-1/2} \;=\; \frac{1}{2}\left[4\tan\left(\frac{\vartheta_j}{4}\right)\hat{\mathbf{u}}_j\right] \circ \frac{1}{2}(\hat{\mathsf{q}}_{j-1/2} + \hat{\mathsf{q}}_{j+1/2})\,. \tag{3}$$

of the equivalent derivative equation $\mathrm{d}\hat{\mathsf{q}}_p = \frac{1}{2}\boldsymbol{\kappa}\circ\hat{\mathsf{q}}$ is obtained by starting from the rotation $\hat{\mathsf{w}}_j = \exp(\vartheta_j/2\,\hat{\mathbf{u}}_j) = \hat{\mathsf{q}}_{j+1/2}\circ\hat{\mathsf{q}}^*_{j-1/2}$ and proceeding in an analogous manner, with the spatial Darboux vector given by $\boldsymbol{\kappa} = \hat{\mathsf{q}}\circ\mathbf{K}\circ\hat{\mathsf{q}}^*$. The FD formula for the spatial Darboux vector $\boldsymbol{\kappa}$ implied by (3) results from a forward rotation $\hat{\mathbf{u}}_j = \hat{\mathsf{q}}_{j\pm1/2}\circ\hat{\mathbf{U}}_j\circ\hat{\mathsf{q}}^*_{j\pm1/2}$ of the material rotation axis to the spatial one, consistent with the FD approximation of the material Darboux vector $\mathbf{K}(p_j)$ implicitely given by (2). Note that the geodesic (*SLERP*) interpolation [35] of the quaternion frames $\hat{\mathsf{q}}_{j\pm1/2}$ on S^3, evaluated at the center of the circular arc connecting $\hat{\mathsf{q}}_{j\pm1/2}$, results in the vertex based quaternion frame $\hat{\mathsf{q}}_j = \bar{\mathsf{p}}_j/|\bar{\mathsf{p}}_j|$ computable by normalizing the *averaged quaternion* $\bar{\mathsf{p}}_j := \frac{1}{2}(\hat{\mathsf{q}}_{j-1/2} + \hat{\mathsf{q}}_{j+1/2})$ appearing on the r.h.s. of both difference equations (2) and (3) to unit length.

The principal theorem for discrete Cosserat curves A unique solution of (2) is obtained by prescribing an initial value $\hat{\mathsf{q}}_{1/2} := \hat{\mathsf{q}}_0 \in S^3$ for the multiplicative iteration, which yields: $\hat{\mathsf{q}}_{j-1/2} = \hat{\mathsf{q}}_0 \circ \prod_{i=1}^{j-1}\hat{\mathsf{W}}_i$.

By construction the definition of $\boldsymbol{\Gamma}_{j-1/2}$ can be reformulated equivalently in terms of the difference equation

$$(p_j - p_{j-1})/\Delta\varsigma_{j-1/2} \;=\; \hat{\mathsf{q}}_{j-1/2}\circ\boldsymbol{\Gamma}_{j-1/2}\circ\hat{\mathsf{q}}^*_{j-1/2} \tag{4}$$

for the vertices of the discrete Cosserat curve centered at $\bar{p}_{j-1/2}$. In the continuum limit $\Delta\varsigma_{j-1/2} = \ell_{j-1/2} \to 0$, the expressions on both sides of (4) converge to $\mathrm{d}p(p) = \hat{\mathsf{q}}(p)\circ\boldsymbol{\Gamma}(p)\circ\hat{\mathsf{q}}^*(p) = \mathbf{t}(p)$ evaluated at $p = p_{j-1/2}$. Obviously, the difference equation (4) can be exactly solved by summation:

$$p_j - p_0 \;=\; \sum_{i=1}^{j}\ell_{i-1/2}\,\mathbf{t}_{i-1/2} \;=\; \sum_{i=1}^{j}\Delta\varsigma_{i-1/2}\,\hat{\mathsf{q}}_{i-1/2}\circ\boldsymbol{\Gamma}_{i-1/2}\circ\hat{\mathsf{q}}^*_{i-1/2}\,. \tag{5}$$

In the continuum limit, this *discrete integration* formula converges to $p_j - p_0 = \int_{p_0}^{p_j}\hat{\mathsf{q}}(p)\circ\boldsymbol{\Gamma}(p)\circ\hat{\mathsf{q}}^*(p)$ with 2^{nd} order accuracy, as the sum corresponds to an approximation of the integral by midpoint quadrature. Using the explicit expression $\hat{\mathsf{q}}_{j-1/2} = \hat{\mathsf{q}}_0\circ\prod_{i=1}^{j-1}\hat{\mathsf{W}}_i$ with $\hat{\mathsf{W}}_i = \exp(\Delta\varsigma_i/2\,\mathbf{K}_i)$, it can be rewritten equivalently in the form

$$p_j \;=\; p_0 + \hat{\mathsf{q}}_0\circ\left[\sum_{i=1}^{j}\Delta\varsigma_{i-1/2}\left(\prod_{m=1}^{i-1}\exp(\Delta\varsigma_m/2\,\mathbf{K}_m)\right)\circ\boldsymbol{\Gamma}_{i-1/2}\circ\left(\prod_{m=1}^{i-1}\exp(\Delta\varsigma_m/2\,\mathbf{K}_m)\right)^*\right]\circ\hat{\mathsf{q}}^*_0\,, \tag{6}$$

which explicitely shows the dependence of the solution on the initial values and discrete invariants.

In eqns. (4), (5) and (6) we may replace the points $p_j = \mathscr{O} + \mathbf{r}_j$ by their position vectors $\mathbf{r}_j$ relative to the origin $\mathscr{O}$ of $\mathscr{E}^3$. The vectors $\mathbf{v}_j := \sum_{i=1}^{j}\Delta\varsigma_{i-1/2}\left(\prod_{m=1}^{i-1}\hat{\mathsf{W}}_m\right)\circ\boldsymbol{\Gamma}_{i-1/2}\circ\left(\prod_{m=1}^{i-1}\hat{\mathsf{W}}_m\right)^*$ point to the postions of the vertices $\{v_j\}_{j=0,\ldots,N}$ of the unique solution of the discrete derivative equations (4) for the inital value $v_0 := \mathscr{O}$,

[4]The notation $(1+\mathbf{q})/(1-\mathbf{q})$ captures the fact that $(1+\mathbf{q})\circ(1-\mathbf{q})^{-1} = (1-\mathbf{q})^{-1}\circ(1+\mathbf{q})$ holds for all $\mathbf{q}\in\mathbb{E}^3$. Likewise the identity $(\hat{\mathsf{p}}-1)\circ(\hat{\mathsf{p}}+1)^{-1} = (\hat{\mathsf{p}}+1)^{-1}\circ(\hat{\mathsf{p}}-1)$ valid for all $-1\neq\hat{\mathsf{p}}\in S^3$ is abbreviated by $(\hat{\mathsf{p}}-1)/(\hat{\mathsf{p}}+1)$.

using the unique solution $\{\hat{\pi}_{j-1/2} := \prod_{m=1}^{j-1} \hat{\mathsf{W}}_m\}_{j=1,\dots,N}$ of the discrete frame equations (2) for the inital value $\hat{\pi}_{1/2} := \hat{1}$. Therefore we may rewrite (6) equivalently as $\mathbf{r}_j - \mathbf{r}_0 = \hat{\mathsf{q}}_0 \circ \mathbf{v}_j \circ \hat{\mathsf{q}}_0^* = \mathsf{R}_0 \cdot \mathbf{v}_j$, where $\mathsf{R}_0 = \mathfrak{E}(\hat{\mathsf{q}}_0)$. As $\hat{\mathsf{q}}_{j-1/2} = \hat{\mathsf{q}}_0 \circ \hat{\pi}_{j-1/2}$ solves (2) for $\hat{\mathsf{q}}_{1/2} := \hat{\mathsf{q}}_0$ and $\mathsf{R}_{j-1/2} = \mathfrak{E}(\hat{\mathsf{q}}_{j-1/2}) = \mathsf{R}_0 \cdot \mathfrak{E}(\hat{\pi}_{j-1/2})$, the general solution of (2), (4) is obtained from the special solution by the operation of the Lie groups $\mathbb{E}^3 \rtimes S^3$ or $SE(3) = \mathbb{E}^3 \rtimes \mathsf{SO}(3)$ on frames in Euclidean space. Note that the latter holds likewise in the continuum setting, which underlines the *mimetic* character of our discrete model.

If we consider the discrete arc length parameters $\{\varsigma_j\}_{j=0,\dots,N}$, the material curvature vectors $\{\mathbf{K}_j\}_{j=1,\dots,N-1}$ and the material tangent vectors $\{\mathbf{\Gamma}_{j-1/2}\}_{j=1,\dots,N}$ as given invariant data of a discrete Cosserat curve, our results outlined above show that we are able to formulate a discrete analogon of the *principal theorem for Cosserat curves*, stating that these data determine the vertices $\{p_j\}_{j=0,\dots,N}$ and quaternion frames $\{\hat{\mathsf{q}}_{j-1/2}\}_{j=1,\dots,N}$ of a discrete Cosserat curve as exact solutions of the discrete derivative equations (2) and (4) up to the arbitrary choice of an initial value $(p_0, \hat{\mathsf{q}}_0) \in \mathscr{E}^3 \times S^3$, corresponding to a global rigid body motion, where the general solution is obtained from the special one determined by $(p_0, \hat{\mathsf{q}}_0) := (\mathscr{O}, \hat{1})$ by the operation of the Lie group of rigid motions in Euclidean space. This statement adresses the essential geometric and kinematical properties of Cosserat curves immersed into Euclidean space. It holds for arbitrary discretizations, and in particular for arbitrary relative rotation angles $\vartheta_j \in [0, 2\pi)$, which leads to favourable properties of discrete Cosserat rod models constructed on this kinematical basis within the variational framework of *(semi)discrete Lagrangian mechanics* [24, 25].

4 Discrete vertex based Cosserat curves and geodesic interpolation in $\mathsf{SE}(3)$

The relation of the discrete Cosserat rod model, based on the discrete kinematics as sketched in the previous section, to the standard approaches to Cosserat rods, using nonlinear finite elements (see eg. [14, 19, 22]), as well as to more recent (and less standard) approaches within the *Lie group* setting [37, 38], using an interpolation of nodal variables using *helicoidal shape functions* [13] with element-wise constant strains [18], is an interesting subject which provides fresh insights into the different approaches.

Kinematics of discrete vertex based Cosserat curves The subject may be investigated most straightforwardly by switching to a vertex based model variant using pairs $(\mathbf{r}_j, \mathsf{R}_j)$ of position vectors $\mathbf{r}_j = \mathbf{x}(p_j) \in \mathbb{E}^3$ and rotation matrices $\mathsf{R}_j = \mathfrak{E}(\hat{\mathsf{q}}_j) \in \mathsf{SO}(3)$ as nodal variables, representing pairs $(p_j, \hat{\mathsf{q}}_j) \in \mathscr{E}^3 \times S^3$ of vertex points p_j and associated unit quaternion frames $\hat{\mathsf{q}}_j = \hat{\mathsf{q}}(p_j)$.

The kinematical description of the rotational variables and the related definition of discrete curvatures can be transfered from the edge based model by shifting indices from half integer to adjacent integer values (and vice versa), such that the material curvature vectors $\mathbf{K}_{j-1/2} := 2\log(\hat{\mathsf{W}}_{j-1/2})/\ell_{j-1/2} = (\vartheta_{j-1/2}/\ell_{j-1/2})\,\hat{\mathbf{U}}_{j-1/2}$ of the vertex based model become edge based quantities, associated to the difference rotations

$$\hat{\mathsf{q}}_{j-1}^* \circ \hat{\mathsf{q}}_j \;=:\; \hat{\mathsf{W}}_{j-1/2} \;=\; \cos(\vartheta_{j-1/2}/2) + \sin(\vartheta_{j-1/2}/2)\,\hat{\mathbf{U}}_{j-1/2} \;=\; \exp(\vartheta_{j-1/2}/2\,\hat{\mathbf{U}}_{j-1/2}) \tag{7}$$

connecting pairs $(\hat{\mathsf{q}}_{j-1}, \hat{\mathsf{q}}_j)$ of adjacent quaternion frames. For given $\mathbf{K}_{j-1/2}$ the iterative update $\hat{\mathsf{q}}_{j-1} \mapsto \hat{\mathsf{q}}_j = \hat{\mathsf{q}}_{j-1} \circ \exp(\ell_{j-1/2}\mathbf{K}_{j-1/2})$ yields the general solution of the finite difference equation

$$2\,(\hat{\mathsf{q}}_j - \hat{\mathsf{q}}_{j-1}) \;=\; \frac{1}{2}(\hat{\mathsf{q}}_{j-1} + \hat{\mathsf{q}}_j) \circ \left[4\tan\left(\frac{\vartheta_{j-1/2}}{4}\right)\hat{\mathbf{U}}_{j-1/2}\right] \tag{8}$$

centered at $p_{j-1/2} \approx \bar{p}_{j-1/2}$, with the unique solution $\{\hat{\mathsf{q}}_j\}_{j=0,\dots,N}$ of (8) for $\hat{\mathsf{q}}_0 \in S^3$ specified as initial value of the iteration given by: $\hat{\mathsf{q}}_j = \hat{\mathsf{q}}_0 \circ \prod_{i=1}^{j} \hat{\mathsf{W}}_{i-1/2}$.

For vertex based frames, the approximation of the integral $\int_{p_{j-1}}^{p_j} \hat{\mathsf{q}}(p) \circ \mathbf{\Gamma}(p) \circ \hat{\mathsf{q}}^*(p) = p_j - p_{j-1}$ by midpoint quadrature is obtained in terms of *edge centered* rotational quaternions $\bar{\mathsf{q}}_{j-1/2} := (\hat{\mathsf{q}}_{j-1} + \hat{\mathsf{q}}_j)/|\hat{\mathsf{q}}_{j-1} + \hat{\mathsf{q}}_j| \in S^3$, defined as averages of adjacent vertex based quaternions normalized to unit length, and a modified definition of the material tangent vectors as $\bar{\mathbf{\Gamma}}_{j-1/2} := \bar{\mathsf{q}}_{j-1/2}^* \circ \mathbf{t}_{j-1/2} \circ \bar{\mathsf{q}}_{j-1/2} = \bar{\mathsf{R}}_{j-1/2}^T \cdot \mathbf{t}_{j-1/2}$, where $\bar{\mathsf{R}}_{j-1/2} := \mathfrak{E}(\bar{\mathsf{q}}_{j-1/2})$. This

leads to a modified discrete derivative equation

$$(p_j - p_{j-1})/\ell_{j-1/2} \;=\; \bar{\mathsf{q}}_{j-1/2} \circ \bar{\boldsymbol{\Gamma}}_{j-1/2} \circ \bar{\mathsf{q}}^*_{j-1/2} \tag{9}$$

that is exactly solved by the discrete integration formula $p_j - p_0 = \sum_{i=1}^{j} \ell_{i-1/2}\, \bar{\mathsf{q}}_{i-1/2} \circ \bar{\boldsymbol{\Gamma}}_{i-1/2} \circ \bar{\mathsf{q}}^*_{i-1/2}$ which yields the vertices of the discrete Cosserat curve in terms of the nodal values of the quaternion frames and the material tangent vectors. Note that $\bar{\mathsf{q}}_{j-1/2}$ and likewise $\bar{\mathsf{R}}_{j-1/2} = \mathfrak{E}(\bar{\mathsf{q}}_{j-1/2})$ are exactly equal to the result of a *geodesic interpolation* of the adjacent nodal quaternions $(\hat{\mathsf{q}}_{j-1}, \hat{\mathsf{q}}_j)$ on S^3, known as *spherical linear interpolation (SLERP)* [35], and nodal frames $(\mathsf{R}_{j-1}, \mathsf{R}_j)$ on $\mathsf{SO}(3)$ (as proposed in [19]), evaluated at the midpoint of the interpolation interval, such that $\bar{\boldsymbol{\Gamma}}_{j-1/2}$ equals the material vector used within the finite element approach to Cosserat rods in the *reduced integration* procedure of terms involving transverse shear strains in the case of a piecewise linear interpolation of nodal position vectors — i.e.: the approximation of the centerline curve by a polygonal arc as sketched in Fig. 3 — to prevent shear locking.

The *principal theorem for discrete vertex based Cosserat curves* then states that the discrete arc length parameters $\{\varsigma_j\}_{j=0,\dots,N}$, the material curvature vectors $\{\mathbf{K}_{j-1/2}\}_{j=1,\dots,N}$ and the material tangent vectors $\{\bar{\boldsymbol{\Gamma}}_{j-1/2}\}_{j=1,\dots,N}$ are the discrete invariant data that determine its configuration $\{(p_j, \hat{\mathsf{q}}_j)\}_{j=0,\dots,N}$ as solution of the discrete derivative equations (8) and (9) up to an overall rigid body motion, corresponding to an arbitrary choice of initial values $(p_0, \hat{\mathsf{q}}_0) \in \mathscr{E}^3 \times S^3$. If we denote the solution of (8) for the inital value $\hat{1}$ by $\hat{\boldsymbol{\pi}}_j$, then $\hat{\mathsf{q}}_j = \hat{\mathsf{q}}_0 \circ \hat{\boldsymbol{\pi}}_j$ is the corresponding solution for arbitrary $\hat{\mathsf{q}}_0 \in S^3$. As $\bar{\mathsf{q}}_{i-1/2} = \hat{\mathsf{q}}_0 \circ \bar{\boldsymbol{\pi}}_{i-1/2}$ holds, we may rewrite the sum formula for the vertices in equivalent form as $p_j - p_0 = \hat{\mathsf{q}}_0 \circ \left[\sum_{i=1}^{j} \ell_{i-1/2}\, \bar{\boldsymbol{\pi}}_{i-1/2} \circ \bar{\boldsymbol{\Gamma}}_{i-1/2} \circ \bar{\boldsymbol{\pi}}^*_{i-1/2}\right] \circ \hat{\mathsf{q}}^*_0$, such that the general solution is again given by the operation of $\mathbb{E}^3 \rtimes S^3$ on the special solution obtained for the inital values $(p_0, \hat{\mathsf{q}}_0) = (\mathscr{O}, \hat{1})$.

Representation of $\mathsf{SE}(3)$ elements by homogeneous transformation matrices in $\mathsf{SL}(4,\mathbb{R})$ The mapping

$$\mathbb{E}^3 \times \mathsf{SO}(3) \ni (\mathbf{c}, \mathsf{Q}) \;\mapsto\; \mathscr{H}(\mathbf{c}, \mathsf{Q}) := \begin{pmatrix} \mathsf{Q} & \mathbf{c} \\ \mathbf{0}^T & 1 \end{pmatrix} \in \mathsf{SL}(4,\mathbb{R}) \tag{10}$$

provides an embedding of $\mathsf{SE}(3)$ into the matrix Lie group $\mathsf{SL}(4,\mathbb{R})$, with matrix multiplication in $\mathsf{SL}(4,\mathbb{R})$ resulting in the group operation of $\mathsf{SE}(3)$ according to the identity $\mathscr{H}(\mathbf{c}_1, \mathsf{Q}_1) \cdot \mathscr{H}(\mathbf{c}_2, \mathsf{Q}_2) = \mathscr{H}(\mathbf{c}_1 + \mathsf{Q}_1 \cdot \mathbf{c}_2, \mathsf{Q}_1 \cdot \mathsf{Q}_2)$. Therefore one may consider frame equations for parameter curves $s \mapsto \mathsf{H}(s) := \mathscr{H}(\mathbf{c}(s), \mathsf{Q}(s))$ in $\mathsf{SL}(4,\mathbb{R})$ in close analogy to frame equations $\partial_s \mathsf{R} = \mathsf{R} \cdot \tilde{\mathsf{K}}$ in $\mathsf{SO}(3)$. The corresponding frame equation for homogeneous transformation matrices $\mathsf{H}(s) = \left(\begin{smallmatrix} \mathsf{R}(s) & \mathbf{r}(s) \\ \mathbf{0}^T & 1 \end{smallmatrix}\right) \in \mathsf{SE}(3)$ reads: $\partial_s \mathsf{H}(s) = \mathsf{H}(s) \cdot \tilde{\mathsf{h}}(s)$. The *left–invariant* vector field $\tilde{\mathsf{h}}(s) := \mathsf{H}^{-1}(s) \cdot \partial_s \mathsf{H}(s) = \left(\begin{smallmatrix} \tilde{\mathsf{K}}(s) & \boldsymbol{\Gamma}(s) \\ \mathbf{0}^T & 0 \end{smallmatrix}\right) \in \mathfrak{se}(3)$ appearing on the r.h.s. of the frame equation is obtained by left multiplication of the derivative $\partial_s \mathsf{H} = \left(\begin{smallmatrix} \partial_s \mathsf{R} & \partial_s \mathbf{r} \\ \mathbf{0}^T & 0 \end{smallmatrix}\right)$ with the inverse $\mathsf{H}^{-1} = \left(\begin{smallmatrix} \mathsf{R}^T & -\mathsf{R}^T \cdot \mathbf{r} \\ \mathbf{0}^T & 1 \end{smallmatrix}\right)$. The fact that $\tilde{\mathsf{h}}(s)$ contains exactly the differential invariants $\tilde{\mathsf{K}} = \mathsf{R}^T \cdot \partial_s \mathsf{R}$ and $\boldsymbol{\Gamma} = \mathsf{R}^T \cdot \partial_s \mathbf{r}$ of the Cosserat curve indicates the kinematical nature of a Cosserat curve as a path in the Lie group $\mathsf{SE}(3)$, with its elements $(\mathbf{r}, \mathsf{R})$ represented by homogeneous transformation matrices $\mathsf{H} = \mathscr{H}(\mathbf{r}, \mathsf{R}) = \left(\begin{smallmatrix} \mathsf{R} & \mathbf{r} \\ \mathbf{0}^T & 1 \end{smallmatrix}\right)$.

The frame equations $\partial_s \mathsf{H}(s) = \mathsf{H}(s) \cdot \tilde{\mathsf{h}}(s)$ are equivalent to the standard derivative equations $\partial_s \mathsf{R} = \mathsf{R} \cdot \tilde{\mathsf{K}}$ in $\mathsf{SO}(3)$ and $\partial_s \mathbf{r} = \mathsf{R} \cdot \boldsymbol{\Gamma}$ in $\mathbb{E}^3$. While the first set corresponds to the (generalized) Frenet equations for the frame directors reformulated for $\mathsf{SO}(3)$ variables, the second set corresponds to the definition of $\boldsymbol{\Gamma}(s)$ solved for the tangent vector of the centerline curve. Thus, the solution procedure for the $\mathsf{SE}(3)$ frame equations *exactly* follows the procedure applied in the constructive proof of the principal theorem for Cosserat curves: First the ODE $\partial_s \mathsf{R} = \mathsf{R} \cdot \tilde{\mathsf{K}}$ is solved for a given material curvature function $\tilde{\mathsf{K}}(s) \in \mathfrak{so}(3)$ and an arbitrarily chosen initial value $\mathsf{R}_0 \in \mathsf{SO}(3)$, with the general solution given by $\mathsf{R}(s; \mathsf{R}_0) = \mathsf{R}_0 \cdot \mathsf{R}(s; \mathsf{I})$, where $\mathsf{R}(s; \mathsf{I})$ is the unique solution for the initial value $\mathsf{R}_0 = \mathsf{I}$. Then the centerline curve can be obtained by subsequent integration for given $\boldsymbol{\Gamma}(s)$, known $\mathsf{R}(s; \mathsf{R}_0)$ and an arbitrarily chosen initial value $\mathbf{r}_0 = \mathbf{r}(s_0)$ as: $\mathbf{r}(s; \mathbf{r}_0) = \mathbf{r}_0 + \mathsf{R}_0 \cdot \int_{s_0}^{s} \mathsf{R}(\zeta; \mathsf{I}) \cdot \boldsymbol{\Gamma}(\zeta)\, d\zeta$. Obviously, the general solution for arbitrary initial values can be generated from the special solution for initial values $(\mathbf{0}, \mathsf{I})$ by means of $\mathsf{SE}(3)$ transformations according to: $\mathscr{H}(\mathbf{r}(s; \mathbf{r}_0), \mathsf{R}(s; \mathsf{R}_0)) = \mathscr{H}(\mathbf{r}_0, \mathsf{R}_0) \cdot \mathscr{H}(\mathbf{r}(s; \mathbf{0}), \mathsf{R}(s; \mathsf{I}))$. This defines a

mapping between parameter curves in $\mathsf{SE}(3)$ that is consistent with the group structure, which underlines the kinematical properties of Cosserat curves as parmeter curves in $\mathsf{SE}(3)$ rather than in the direct product $\mathbb{E}^3 \times \mathsf{SO}(3)$. However, one may likewise consider this mapping as an operation of the group $\mathsf{SE}(3)$ on elements of (and likewise parameter curves in) the manifold $\mathbb{E}^3 \times \mathsf{SO}(3)$.

Geodesic interpolation in $\mathbb{E}^3 \times \mathsf{SO}(3)$ and $\mathsf{SE}(3)$ While $\mathbb{E}^3 \times \mathsf{SO}(3)$ and $\mathsf{SE}(3) = \mathbb{E}^3 \rtimes \mathsf{SO}(3)$ are equal as sets, they are *not* equal as Lie groups, as the group operations definied on both sets are *different*. This influences also the *metric* properties of both groups, considered as Riemannian manifolds.

In the case of the direct product $\mathbb{E}^3 \times \mathsf{SO}(3)$ the geodesics are just the well known ones of the uncoupled factors, i.e.: straight line segments connecting vertex positions in $\mathbb{E}^3$ according to

$$[\zeta_j, \zeta_{j+1}] \ni \zeta \;\mapsto\; \mathbf{r}(\zeta) := \mathbf{r}_j + (\zeta - \zeta_j)\,\frac{\mathbf{r}_{j+1} - \mathbf{r}_j}{\zeta_{j+1} - \zeta_j}\,, \tag{11}$$

combined with constant curvature paths in $\mathsf{SO}(3)$, corresponding to great circular arcs on S^3, that are obtained from the (*SLERP*–equivalent) interpolation formula

$$[\zeta_j, \zeta_{j+1}] \ni \zeta \;\mapsto\; \mathsf{R}(\zeta) := \mathsf{R}_j \cdot \exp_{SO(3)}\left(\frac{\zeta - \zeta_j}{\zeta_{j+1} - \zeta_j}\,\tilde{\vartheta}_{j+1/2}\right)\,, \tag{12}$$

where $\exp_{SO(3)}(\tilde{\vartheta}_{j+1/2}) = \mathsf{R}_j^T \cdot \mathsf{R}_{j+1}$, i.e.: $\tilde{\vartheta}_{j+1/2} := \log_{SO(3)}\left(\mathsf{R}_j^T \cdot \mathsf{R}_{j+1}\right) =: (\zeta_{j+1} - \zeta_j)\,\tilde{\mathsf{K}}_{j+1/2} \in \mathfrak{so}(3)$.

The geodesics in $\mathsf{SE}(3)$ result from an interpolation procedure that mimics constant curvature (*SLERP*) interpolation of rotations in $\mathsf{SO}(3)$, i.e.:

$$[\zeta_j, \zeta_{j+1}] \ni \zeta \;\mapsto\; \mathsf{H}(\zeta) := \mathsf{H}_j \cdot \exp_{SE(3)}\left(\frac{\zeta - \zeta_j}{\zeta_{j+1} - \zeta_j}\,\tilde{\Psi}_{j+1/2}\right)\,, \tag{13}$$

where $\exp_{SE(3)}(\tilde{\Psi}_{j+1/2}) = \mathsf{H}_j^{-1} \cdot \mathsf{H}_{j+1}$, i.e.: $\tilde{\Psi}_{j+1/2} := \log_{SE(3)}\left(\mathsf{H}_j^{-1} \cdot \mathsf{H}_{j+1}\right) =: (\zeta_{j+1} - \zeta_j)\,\tilde{\mathsf{h}}_{j+1/2} \in \mathfrak{se}(3)$. So, geodesic interpolation in $\mathsf{SE}(3)$ connects pairs $(\mathsf{H}_j, \mathsf{H}_{j+1})$ of adjacent frames by curves of constant $\tilde{\mathsf{h}}_{j+1/2}$, where $\tilde{\mathsf{h}}_{j+1/2} = \begin{pmatrix} \tilde{\mathsf{K}}_{j+1/2} & \mathbf{\Gamma}_{j+1/2} \\ \mathbf{0}^T & 0 \end{pmatrix} = \tilde{\Psi}_{j+1/2}/(\zeta_{j+1} - \zeta_j)$. By construction the constant material curvature is given by the already known formula $\tilde{\mathsf{K}}_{j+1/2} = \tilde{\vartheta}_{j+1/2}/(\zeta_{j+1} - \zeta_j)$, where $\tilde{\vartheta}_{j+1/2} = \log_{SO(3)}\left(\mathsf{R}_j^T \cdot \mathsf{R}_{j+1}\right)$. The exact expression for $\mathbf{\Gamma}_{j+1/2}$ as a function of the adjacent frames is more complicated and will be derived below.

Helix–shaped centerline curves For constant $\tilde{\mathsf{K}}_{j+1/2}$ and $\mathbf{\Gamma}_{j+1/2}$ the centerline curved may be computed explicitely in analytically closed form. In the interval $[\zeta_j, \zeta_{j+1}]$ the centerline curve is given by $\mathbf{r}(\zeta) = \mathbf{r}_j + \mathsf{R}_j \cdot \int_{\zeta_j}^{\zeta} d\xi\, \exp\left(\frac{\xi - \zeta_j}{\zeta_{j+1} - \zeta_j}\,\tilde{\vartheta}_{j+1/2}\right) \cdot \mathbf{\Gamma}_{j+1/2}$. With the definitions $\vartheta_{j+1/2} := \|\tilde{\vartheta}_{j+1/2}\|$, $\hat{\vartheta}_{j+1/2} := \tilde{\vartheta}_{j+1/2}/\|\tilde{\vartheta}_{j+1/2}\|$, $\tilde{\mathsf{K}}_{j+1/2} := \tilde{\vartheta}_{j+1/2}/(\zeta_{j+1} - \zeta_j)$ and $K_{j+1/2} := \|\tilde{\mathsf{K}}_{j+1/2}\| = \vartheta_{j+1/2}/(\zeta_{j+1} - \zeta_j)$ we may rewrite the integral formula for the interpolation of the centerline curve equivalently as: $\mathsf{R}_j^T \cdot [\mathbf{r}(\zeta) - \mathbf{r}_j] = \int_0^{\zeta - \zeta_j} ds\, \exp(s K_{j+1/2}\,\hat{\vartheta}_{j+1/2}) \cdot \mathbf{\Gamma}_{j+1/2}$. Inserting the *Euler–Rodrigues formula* $\exp(\tilde{\Omega}) = \mathsf{I} + \sin(\Omega)\hat{\Omega} + [1 - \cos(\Omega)]\,\hat{\Omega}^2$ for $\tilde{\Omega} \in \mathfrak{so}(3)$ with norm $\Omega := \|\tilde{\Omega}\|$ and $\mathfrak{so}(3) \ni \hat{\Omega} := \tilde{\Omega}/\Omega \Rightarrow \|\hat{\Omega}\| = 1$, the integral involving the exponential function of $\mathsf{SO}(3)$ may be computed in closed form, with the result:

$$\mathsf{R}_j^T \cdot [\mathbf{r}(\zeta) - \mathbf{r}_j] \;=\; \Delta\zeta \left\{ \mathsf{I} + \frac{1 - \cos(\Delta\zeta K_{j+1/2})}{\Delta\zeta K_{j+1/2}}\,\hat{\vartheta}_{j+1/2} + \frac{\Delta\zeta K_{j+1/2} - \sin(\Delta\zeta K_{j+1/2})}{\Delta\zeta K_{j+1/2}}\,\hat{\vartheta}_{j+1/2}^2 \right\} \cdot \mathbf{\Gamma}_{j+1/2}\,. \tag{14}$$

By inspection (and some elementary vector algebra) one can show that the interpolated centerline curve $\zeta \mapsto \mathbf{r}(\zeta)$ given by (14) for $\zeta \in [\zeta_j, \zeta_{j+1}]$ is a helix.

Exact and approximate expressions for the material tangent vector field *Helicoidal interpolation* as discussed in the previous paragraph starts at given constant invariants $\mathbf{K}_{j+1/2}$ and $\mathbf{\Gamma}_{j+1/2}$ and provides parametrized curve segments $\zeta \mapsto (\mathbf{r}(\zeta), \mathsf{R}\zeta)$ for each interval $[\zeta_j, \zeta_{j+1}]$ starting at initial values $(\mathbf{r}_j, \mathsf{R}_j)$ and terminating at final values $(\mathbf{r}_{j+1}, \mathsf{R}_{j+1})$, with $\mathbf{r}_{j+1} = \mathbf{r}(\zeta_{j+1})$ and $\mathsf{R}_{j+1} = \mathsf{R}(\zeta_{j+1})$. If one aims at computing the interpolating helical curve segments for a set $\{(\mathbf{r}_j, \mathsf{R}_j)\}_{j=0,\dots,n} \subset \mathbb{E}^3 \times \mathsf{SO}(3)$ of given vertex data, one needs to extract the segment-wise constant invariants $\mathbf{K}_{j+1/2}$ and $\mathbf{\Gamma}_{j+1/2}$ from the respective frames $(\mathbf{r}_j, \mathsf{R}_j)$ and $(\mathbf{r}_{j+1}, \mathsf{R}_{j+1})$ as input for the interpolation formulas.

For the material curvature vector the geodesic interpolation formula (12) can be inverted to compute $\tilde{\vartheta}_{j+1/2} = \log_{SO(3)}\left(\mathsf{R}_j^T \cdot \mathsf{R}_{j+1}\right) = (\zeta_{j+1} - \zeta_j)\,\tilde{\mathsf{K}}_{j+1/2} \in \mathfrak{so}(3)$, which formally solves the task for the rotational part. In practise one considers the material difference rotation $\mathsf{W}_{j+1/2} = \mathsf{R}_j^T \cdot \mathsf{R}_{j+1}$ and utilize the Euler–Rodrigues formula to compute the terms $\mathsf{W}_{j+1/2} - \mathsf{W}_{j+1/2}^T = 2\sin(\vartheta_{j+1/2})\hat{\vartheta}_{j+1/2}$ and $2\cos(\vartheta_{j+1/2}) = \mathrm{Tr}\left(\mathsf{W}_{j+1/2}\right) - 1$, which may be combined e.g. to the identity $(\mathsf{W}_{j+1/2} - \mathsf{W}_{j+1/2}^T)/(\mathrm{Tr}\left(\mathsf{W}_{j+1/2}\right) + 1) = \tan(\vartheta_{j+1/2}/2)\hat{\vartheta}_{j+1/2}$. The latter relation results identically from the inverse Cayley transform $(\mathsf{W}_{j+1/2} + \mathsf{I}) \cdot (\mathsf{W}_{j+1/2} - \mathsf{I})^{-1} =: \mathrm{cay}^{-1}(\mathsf{W}_{j+1/2})$ of the material difference rotation. Using these identities one can extract both the normalized rotation axis $\hat{\vartheta}_{j+1/2}$ and a positive rotation angle $\vartheta_{j+1/2} \in (0, 2\pi)$, and finally compute the desired result $\tilde{\vartheta}_{j+1/2} = \vartheta_{j+1/2}\,\hat{\vartheta}_{j+1/2}$, formally obtained from the logarithm on $\mathsf{SO}(3)$. If the vertex frames are given by rotational quaternions $\hat{\mathsf{q}}_j$ and $\hat{\mathsf{q}}_{j+1}$ connected by the material difference rotation $\hat{\mathsf{q}}_j^* \circ \hat{\mathsf{q}}_{j+1} =: \hat{\mathsf{W}}_{j+1/2} = \cos(\vartheta_{j+1/2}/2) + \sin(\vartheta_{j+1/2}/2)\,\hat{\mathbf{U}}_{j+1/2}$, one can obtain $\tan(\vartheta_{j+1/2}/2)\,\hat{\mathbf{U}}_{j+1/2}$ or $\tan(\vartheta_{j+1/2}/4)\,\hat{\mathbf{U}}_{j+1/2}$ in terms of simple algebraic expressions[5] of the real and imaginary parts of $\hat{\mathsf{W}}_{j+1/2}$. From these expressions one may again obtain $\hat{\mathbf{U}}_{j+1/2} \simeq \hat{\vartheta}_{j+1/2}$ by normalization, and $\vartheta_{j+1/2} \in [0, 2\pi)$ by applying the $\arctan(\dots)$ function to the terms equal to $\tan(\vartheta_{j+1/2}/2)$ or $\tan(\vartheta_{j+1/2}/4)$. These considerations sketch the pratical approach taken to compute the logarithm on $\mathsf{SO}(3)$ or S^3, respectively.

For the derivation of an explict formula to compute $\mathbf{\Gamma}_{j+1/2}$ from given vertex frame data $(\mathbf{r}_j, \mathsf{R}_j)$ and $(\mathbf{r}_{j+1}, \mathsf{R}_{j+1})$ one may take (14) evaluated at $\zeta = \zeta_{j+1}$ as a starting point, which may be rewritten as

$$\bar{\mathsf{R}}_{j+1/2}^T \cdot \frac{\mathbf{r}_{j+1} - \mathbf{r}_j}{\zeta_{j+1} - \zeta_j} \;=:\; \mathbf{\Gamma}_{j+1/2}^{(r)} \;=\; \int_{-\frac{1}{2}}^{\frac{1}{2}} d\lambda\, \exp\left(\lambda\,\tilde{\vartheta}_{j+1/2}\right) \cdot \mathbf{\Gamma}_{j+1/2} \tag{15}$$

in terms of the edge centered frames $\mathfrak{E}(\bar{\mathsf{q}}_{j+1/2}) =: \bar{\mathsf{R}}_{j+1/2} = \mathsf{R}_j \cdot \exp(\tilde{\vartheta}_{j+1/2}/2) = \mathsf{R}_{j+1} \cdot \exp(-\tilde{\vartheta}_{j+1/2}/2)$ obtained from geodesic interpolation of the vertex frames.

Note that $\mathbf{\Gamma}_{j+1/2}^{(r)} = \ell_{j+1/2}/(\zeta_{j+1} - \zeta_j)\bar{\mathbf{\Gamma}}_{j+1/2}$ (with $\bar{\mathbf{\Gamma}}_{j+1/2} = \bar{\mathsf{R}}_{j+1/2}^T \cdot \mathbf{t}_{j+1/2}$) is equal to the segment-wise constant shear strain measure used in the reduced integration procedure for polygonally interpolated centerline curves in $\mathbb{E}^3$ with a geodesic interpolation of the $\mathsf{SO}(3)$ d.o.f. (i.e.: for geodesic interpolation in $\mathbb{E}^3 \times \mathsf{SO}(3)$).

The integral above can be evaluated analytically and yields the closed form expression

$$\exp\left(-\tilde{\vartheta}/2\right) \cdot \mathsf{G}(\tilde{\vartheta}) \;:=\; \int_{-\frac{1}{2}}^{\frac{1}{2}} d\lambda\, \exp\left(\lambda\,\tilde{\vartheta}\right) \;=\; \mathsf{I} + \left[1 - \frac{2}{\vartheta}\sin\left(\frac{\vartheta}{2}\right)\right] \hat{\vartheta}^2 \;=:\; \mathsf{D}(\tilde{\vartheta}) \tag{16}$$

valid for $\tilde{\vartheta} \in \mathfrak{so}(3)$, $\vartheta = \|\tilde{\vartheta}\|$ and $\hat{\vartheta} = \tilde{\vartheta}/\|\tilde{\vartheta}\|$ with $\vartheta \geq 0$ (as the limit $\vartheta \to 0$ is well defined).

The operator $\mathsf{D}(\tilde{\vartheta}) : \mathbb{E}^3 \to \mathbb{E}^3$ is symmetric and can be inverted for $\vartheta \in [0, 2\pi)$. This can be proved by considering a linear operator of the form $\mathsf{A} = \mathsf{I} + \sigma\hat{\mathsf{N}}^2$ with $\sigma \in \mathbb{R}$ and $\hat{\mathsf{N}} \in \mathfrak{so}(3)$, $\|\hat{\mathsf{N}}\| = 1$. As $\hat{\mathsf{N}}^2 = \hat{\mathbf{N}} \otimes \hat{\mathbf{N}} - \mathsf{I}$ the operator can be equivalently represented by the sum $\mathsf{A} = \hat{\mathbf{N}} \otimes \hat{\mathbf{N}} + (1 - \sigma)[\mathsf{I} - \hat{\mathbf{N}} \otimes \hat{\mathbf{N}}]$ of orthogonal projectors, such that its inverse is given by $\mathsf{A}^{-1} = \hat{\mathbf{N}} \otimes \hat{\mathbf{N}} + (1 - \sigma)^{-1}[\mathsf{I} - \hat{\mathbf{N}} \otimes \hat{\mathbf{N}}] = \mathsf{I} + [\sigma/(\sigma - 1)]\hat{\mathsf{N}}^2$ for $\sigma \neq 1$. The inverse of $\mathsf{D}(\tilde{\vartheta})$ can be obtained by substituting $\hat{\mathsf{N}} = \hat{\vartheta}$ and $\sigma = 1 - (2/\vartheta)\sin(\vartheta/2) \Rightarrow \sigma/(\sigma - 1) = \vartheta/[2\sin(\vartheta/2)]$, with the result:

$$\mathsf{D}(\tilde{\vartheta})^{-1} \;=\; \left\{\mathsf{I} + \left[1 - \frac{2}{\vartheta}\sin\left(\frac{\vartheta}{2}\right)\right] \hat{\vartheta}^2\right\}^{-1} \;=\; \mathsf{I} + \left[1 - \frac{\vartheta}{2\sin(\vartheta/2)}\right] \hat{\vartheta}^2\,, \quad \vartheta \in [0, 2\pi)\,. \tag{17}$$

[5] Note that the second variant may e.g. be obtained by solving (8) for $\tan(\vartheta_{j+1/2}/4)\,\hat{\mathbf{U}}_{j+1/2} = (\hat{\mathsf{q}}_{j+1} + \hat{\mathsf{q}}_j)^{-1} \circ (\hat{\mathsf{q}}_{j+1} - \hat{\mathsf{q}}_j)$, or equivalently by the inverse quaternionic Cayley transform of $\hat{\mathsf{W}}_{j+1/2}$.

We finally obtain the two closed form expressions

$$\boldsymbol{\Gamma}^{(r)}_{j+1/2} \;=\; \mathsf{D}(\tilde{\boldsymbol{\vartheta}}_{j+1/2})\cdot\boldsymbol{\Gamma}_{j+1/2} \;\Leftrightarrow\; \boldsymbol{\Gamma}_{j+1/2} \;=\; \mathsf{D}(\tilde{\boldsymbol{\vartheta}}_{j+1/2})^{-1}\cdot\boldsymbol{\Gamma}^{(r)}_{j+1/2} \tag{18}$$

relating the material vector quantities $\boldsymbol{\Gamma}^{(r)}_{j+1/2}$ and $\boldsymbol{\Gamma}_{j+1/2}$. In particular, the second expression formally yields an explicit formula to compute $\boldsymbol{\Gamma}_{j+1/2}$ in terms of given frame data $(\mathbf{r}_j,\mathsf{R}_j)$ and $(\mathbf{r}_{j+1},\mathsf{R}_{j+1})$, by applying the operator $\mathsf{D}(\tilde{\boldsymbol{\vartheta}}_{j+1/2})^{-1}$, which is a nonlinear function of $\log(\mathsf{R}_j^T\cdot\mathsf{R}_{j+1/2}) = \tilde{\boldsymbol{\vartheta}}_{j+1/2} = \vartheta_{j+1/2}\,\hat{\boldsymbol{\vartheta}}_{j+1/2}$, to the simplified expression $\boldsymbol{\Gamma}^{(r)}_{j+1/2}$. The computational evaluation of this formula requires the substitution of explicit espressions for $\vartheta_{j+1/2}$, $\sin(\vartheta_{j+1/2}/2)$ and $\hat{\boldsymbol{\vartheta}}^2_{j+1/2}$ in terms of $\mathsf{W}_{j+1/2} = \mathsf{R}_j^T\cdot\mathsf{R}_{j+1/2}$. The Taylor expansion $1-(2/\vartheta)\sin(\vartheta/2) = \vartheta^2/24+\mathscr{O}(\vartheta^4)$ yields the estimates $\|\mathsf{D}(\tilde{\boldsymbol{\vartheta}})^{\pm1}-\mathsf{I}\|\approx\vartheta^2/24$, which measure the deviation of $\mathsf{D}(\tilde{\boldsymbol{\vartheta}})$ and its inverse from the identity and likewise quantify the relative deviation of $\boldsymbol{\Gamma}^{(r)}_{j+1/2}$ from $\boldsymbol{\Gamma}_{j+1/2}$.

The logarithm function on $\mathsf{SE}(3)$ revisited As a by-product of the above results we are now able to derive a closed form expression for the vector part of the logarithm on $\mathsf{SE}(3)$. Recall that for a pair of transformation matrices $\mathsf{H}_j = \left(\begin{smallmatrix}\mathsf{R}_j & \mathbf{r}_j\\ \mathbf{0}^T & 1\end{smallmatrix}\right)$ and $\mathsf{H}_{j+1} = \left(\begin{smallmatrix}\mathsf{R}_{j+1} & \mathbf{r}_{j+1}\\ \mathbf{0}^T & 1\end{smallmatrix}\right)$ the constant invariants of the geodesic interpolation curve are obtained as $\tilde{\mathsf{h}}_{j+1/2} = \left(\begin{smallmatrix}\tilde{\mathsf{K}}_{j+1/2} & \boldsymbol{\Gamma}_{j+1/2}\\ \mathbf{0}^T & 0\end{smallmatrix}\right) = \tilde{\boldsymbol{\Psi}}_{j+1/2}/(\zeta_{j+1}-\zeta_j)$, where $\exp_{SE(3)}(\tilde{\boldsymbol{\Psi}}_{j+1/2}) = \mathsf{H}_j^{-1}\cdot\mathsf{H}_{j+1}$ and $\tilde{\boldsymbol{\Psi}}_{j+1/2} = \log_{SE(3)}\left(\mathsf{H}_j^{-1}\cdot\mathsf{H}_{j+1}\right) = (\zeta_{j+1}-\zeta_j)\,\tilde{\mathsf{h}}_{j+1/2}\in\mathfrak{se}(3)$. As $\mathsf{H}_j^{-1}\cdot\mathsf{H}_{j+1} = \left(\begin{smallmatrix}\mathsf{R}_j^T\cdot\mathsf{R}_{j+1} & \mathsf{R}_j^T\cdot(\mathbf{r}_{j+1}-\mathbf{r}_j)\\ \mathbf{0}^T & 1\end{smallmatrix}\right)$, with the vector part of this transformation matrix related to $\boldsymbol{\Gamma}_{j+1/2}$ by $\mathsf{R}_j^T\cdot(\mathbf{r}_{j+1}-\mathbf{r}_j) = (\zeta_{j+1}-\zeta_j)\,\mathsf{G}(\vartheta_{j+1/2})\cdot\boldsymbol{\Gamma}_{j+1/2}$, where $\tilde{\boldsymbol{\vartheta}}_{j+1/2} = \log_{SO(3)}\left(\mathsf{R}_j^T\cdot\mathsf{R}_{j+1}\right) = (\zeta_{j+1}-\zeta_j)\,\tilde{\mathsf{K}}_{j+1/2}$, one recognizes by inspection that the vector part of $\log_{SE(3)}(\ldots)$ can be obtained from the inverse operator $\mathsf{G}(\tilde{\boldsymbol{\vartheta}}_{j+1/2})^{-1}$, such that $(\zeta_{j+1}-\zeta_j)\boldsymbol{\Gamma}_{j+1/2} = \mathsf{G}(\tilde{\boldsymbol{\vartheta}}_{j+1/2})^{-1}\cdot\left[\mathsf{R}_j^T\cdot(\mathbf{r}_{j+1}-\mathbf{r}_j)\right]$ holds identically. Altogether this yields the following operational definition of the logarithm on $\mathsf{SE}(3)$:

$$\mathsf{SE}(3)\ni\begin{pmatrix}\mathsf{Q} & \mathbf{c}\\ \mathbf{0}^T & 1\end{pmatrix}\;\mapsto\;\log_{\mathsf{SE}(3)}\begin{pmatrix}\mathsf{Q} & \mathbf{c}\\ \mathbf{0}^T & 1\end{pmatrix}\;=\;\begin{pmatrix}\log_{SO(3)}(\mathsf{Q}) & \mathsf{G}\left(\log_{SO(3)}(\mathsf{Q})\right)^{-1}\cdot\mathbf{c}\\ \mathbf{0}^T & 0\end{pmatrix}\in\mathfrak{se}(3)\,. \tag{19}$$

The closed form expression $\mathsf{G}(\tilde{\boldsymbol{\vartheta}})^{-1} = \mathsf{D}(\tilde{\boldsymbol{\vartheta}})^{-1}\cdot\exp(-\tilde{\boldsymbol{\vartheta}}/2)$ can be obtained from (16) and (17), with the exponential function inserted from the Euler–Rodrigues formula.

5 Conclusions

We utilized ideas from the *difference geometry of framed curves* [34] to construct the *discrete kinematics* of Cosserat rod models such that essential geometric properties are preserved for arbitrarily coarse discretizations. Consistent with discrete Frenet curve theory, we defined discrete Cosserat curves as polygonal arcs with edge centered frames on a staggered grid. We pointed out how to modify the discrete scheme to obtain a vertex based model variant, as used for both a standard discretization of Cosserat rods with nonlinear finite elements [14, 19, 22] in $\mathbb{E}^3\times\mathsf{SO}(3)$ as well as for geodesic finite elements in $\mathsf{SE}(3)$ with *helicoidal shape functions* [13, 37, 38] and element-wise constant strains [18]. Such vertex based discrete Cosserat rods are conceptually close to the standard finite element formulation in $\mathbb{E}^3\times\mathsf{SO}(3)$, which in turn differs from the formulation using geodesic interpolation in $\mathsf{SE}(3)$ in the shear strains only. We obtained a closed form expression relating the shear strains obtained by reduced integration to the values obtained in helicoidal interpolation and showed that the former approximate the latter up to second order in the relative rotation angle between adjacent nodal frames. Our findings motivate numerical investigations of the different model variants to gain further insight into geometric discretisations of Cosserat rods. It will be interesting to find out whether the *mechanical* properties of helicoidal shape functions, which arise as static equilibria of uniform Cosserat rods [1, 16, 17] and therefore can be interpreted as *mechanical splines*, lead to practical advantages in numerical computations despite their increased algebraic complexity.

A Mathematical basics and notational conventions

In this section we collect a few facts of linear algebra and the calculus of space curves to introduce some notational conventions inspired by the ones given in [2, 23].

Euclidean point space $\mathscr{E}^3$ and its vector space $\mathbb{E}^3$ We denote three–dimensional Euclidean point space by $\mathscr{E}^3$, its associated Euclidian vector space by $\mathbb{E}^3$ and use bracket notation $\langle\cdot,\cdot\rangle$ to denote its scalar product. All vectors $\mathbf{w}\in\mathbb{E}^3$ are written in boldface roman letters. By definition, they provide parallel displacements $q=p+\mathbf{w}$ of points $p,q\in\mathscr{E}^3$. This explains the operation $+:\mathscr{E}^3\times\mathbb{E}^3\to\mathscr{E}^3$ on Euclidian space $\left(\mathscr{E}^3,\mathbb{E}^3,+\right)$ and also defines the difference $q-p=\mathbf{w}$ of points. The distance of points in $\mathscr{E}^3$ is measured by the length $\|\mathbf{w}\|=\sqrt{\langle\mathbf{w},\mathbf{w}\rangle}=:\|q-p\|$ of their displacement vectors. A fixed cartesian coordinate frame of $\mathbb{E}^3$ is defined by choosing a fixed origin $\mathscr{O}=\mathbf{0}$ and a fixed right–handed orthonormal triple $(\mathbf{e}_1,\mathbf{e}_2,\mathbf{e}_3)$ of basis vectors. Any vector quantity may be decomposed with respect to the fixed basis $\{\mathbf{e}_k\}_{k=1,2,3}$ in the form $\mathbf{w}=\sum_{k=1}^3 w_k\mathbf{e}_k$, where the real numbers $w_k=\langle\mathbf{w},\mathbf{e}_k\rangle$ denote the cartesian components of $\mathbf{w}\in\mathbb{E}^3$. The position vector $\mathbf{x}(p)$ of a point $p\in\mathscr{E}^3$ is given by $p=\mathscr{O}+\mathbf{x}(p)$, with its cartesian components $x_k(p)=\langle\mathbf{x}(p),\mathbf{e}_k\rangle$. Any vector quantity may be decomposed with respect to the fixed basis $\{\mathbf{e}_k\}_{k=1,2,3}$ in the form $\mathbf{w}=\sum_{k=1}^3 w_k\mathbf{e}_k$, where the real numbers $w_k=\langle\mathbf{w},\mathbf{e}_k\rangle$ denote the cartesian components of $\mathbf{w}\in\mathbb{E}^3$. In this way one can isomorphically identify abstract vectors $\mathbf{w}\in\mathbb{E}^3$ with the column vectors $(w_1,w_2,w_3)^T\in\mathbb{R}^3$ consisting of their cartesian coefficient triples by mapping the fixed basis vectors $\{\mathbf{e}_k\}_{k=1,2,3}$ to the canonical basis $\{(1,0,0)^T,(0,1,0)^T,(0,0,1)^T\}$ of $\mathbb{R}^3$, which establishes the isomorphism $\mathbb{E}^3\simeq\mathbb{R}^3$ of real vector spaces.

Linear mappings in $\mathbb{E}^3$ We denote linear mappings $\mathsf{A}:\mathbb{E}^3\to\mathbb{E}^3$ within Euclidian vector space by upper case upright serifless letters and use dot notation $\mathbf{w}\mapsto\mathsf{A}\cdot\mathbf{w}$ for their operation on vectors as well as for the composition $(\mathsf{A}\cdot\mathsf{B})\cdot\mathbf{w}=\mathsf{A}\cdot(\mathsf{B}\cdot\mathbf{w})$ of linear mappings. The identity I maps all vectors onto themselves.

A linear mapping is completely determined by its values $\mathbf{v_k}=\mathsf{A}\cdot\mathbf{e}_k$ on the fixed basis and may be written in invariant form as a sum[6] $\mathsf{A}=\sum_{k=1}^3\mathbf{v}_k\otimes\mathbf{e}_k\equiv\mathbf{v}_k\otimes\mathbf{e}_k$ of tensor products defined as $(\mathbf{a}\otimes\mathbf{b})\cdot\mathbf{w}=\langle\mathbf{b},\mathbf{w}\rangle\,\mathbf{a}$. The corresponding representation of the identity in terms of the fixed basis is given by $\mathsf{I}=\mathbf{e}_k\otimes\mathbf{e}_k$. Occasionally we use the notation $\mathsf{A}=(\mathbf{v}_1,\mathbf{v}_2,\mathbf{v}_3)$, which identifies the linear mapping A with the triple of vectors obtained as images of the fixed basis. By definition the components A_{ij} of the 3×3 matrix representing A w.r.t. the fixed basis $\{\mathbf{e}_k\}_{k=1,2,3}$ are given by $A_{ij}=\langle\mathbf{e}_i,\mathsf{A}\cdot\mathbf{e}_j\rangle$. In particular, the components of the identity are given by $\langle\mathbf{e}_i,\mathbf{e}_j\rangle=\delta_{ij}$ (i.e.: *Kronecker's* symbol).

The determinant $\det(\mathsf{A})$ of a linear mapping is an invariant and equals the determinant of its representing matrix w.r.t. an arbitrary basis. The cross product $\mathbf{u}\times\mathbf{v}$ of vectors may be definied invariantly via the identity $\langle\mathbf{u}\times\mathbf{v},\mathbf{w}\rangle=\det((\mathbf{u},\mathbf{v},\mathbf{w}))=[\mathbf{u},\mathbf{v},\mathbf{w}]$ which is required to hold for arbitrary vectors, and likewise explains their scalar valued triple product. The identity $\tilde{\mathbf{u}}\cdot\mathbf{v}=\mathbf{u}\times\mathbf{v}$ establishes the one–to–one correspondence between vectors $\mathbf{u}$ and skew–symmetric mappings $\tilde{\mathbf{u}}=-\tilde{\mathbf{u}}^T$, represented by *tilde notation*.

Rotations and Quaternions Linear mappings that preserve length are denoted as *orthogonal*: for orthogonal mappings R the identity $\|\mathbf{w}\|=\|\mathsf{R}\cdot\mathbf{w}\|$ must holds for all vectors $\mathbf{w}\in\mathbb{E}^3$. This implies the orthonormality $\langle\mathbf{a}_i,\mathbf{a}_j\rangle=\delta_{ij}$ of the column vectors $\mathbf{a}_k=\mathsf{R}\cdot\mathbf{e}_k$ of an orthogonal mapping. This characteristic property may be equivalently formulated in a more compact form by the identities $\mathsf{R}^T=\mathsf{R}^{-1}$ or $\mathsf{R}^T\cdot\mathsf{R}=\mathsf{I}=\mathsf{R}\cdot\mathsf{R}^T$ which hold by definition for any orthogonal mapping. Orthogonal mappings R that preserve the orientation of the fixed basis are characterized by $\det(\mathsf{R})=1$ and denoted as *proper orthogonal*. The orthogonal and proper orthogonal linear mappings on $\mathbb{E}^3$ form Lie groups $\mathsf{O}(3)$ and $\mathsf{SO}(3)$ respectively. Their Lie algebra is the set $\mathfrak{so}(3)\simeq\mathbb{R}^3\simeq\mathbb{E}^3$ of skew–symmetric linear mappings. Both groups are subgroups of the Lie group $\mathsf{GL}(3)$ of invertible linear mappings on $\mathbb{E}^3$ whose Lie algebra is the set $\mathfrak{gl}(3)\simeq\mathbb{R}^9\simeq\mathbb{E}^3\otimes\mathbb{E}^3$ of arbitrary linear mappings (or real 3×3 matrices).

[6] We make frequent use of *Einstein's summation convention*, with latin indices $i,j,k,\ldots$ running from 1 to 3, and greek indices $\alpha,\beta,\ldots$ from 1 to 2.

Following ch. 7 of [21], we denote Hamilton's algebra of *quaternions* by $\mathbb{H}$. We identify the orthonormal basis $\{\mathbf{i},\mathbf{j},\mathbf{k}\}$ of $\Im\mathbb{H} \simeq \mathbb{E}^3$ with the fixed basis $\{\mathbf{e}_1,\mathbf{e}_2,\mathbf{e}_3\}$ of $\mathbb{E}^3$. Denoting the base vector of $\Re\mathbb{H} \simeq \mathbb{R}$ as $\mathbf{e}_0 = 1$, we may represent arbitrary quaternions invariantly as[7] $\mathsf{q} = q + \mathbf{q}$, with scalar part $q = \Re(\mathsf{q}) \in \mathbb{E}^1 \simeq \mathbb{R}$ and vector part $\mathbf{q} = \Im(\mathsf{q}) \in \mathbb{E}^3 \simeq \mathbb{R}^3$. The product of two arbitrary quaternions p and q is given by the formula: $\mathsf{p}\circ\mathsf{q} = pq - \langle\mathbf{p},\mathbf{q}\rangle + p\mathbf{q} + q\mathbf{p} + \mathbf{p}\times\mathbf{q}$. Using the notation $\mathsf{q}^* = q - \mathbf{q}$ for conjugate quaternions, the scalar product $\langle\ ,\ \rangle_{\mathbb{H}}$ of $\mathbb{H} \simeq \mathbb{E}^4$ may be obtained by $\langle\mathsf{p},\mathsf{q}\rangle_{\mathbb{H}} = \frac{1}{2}(\mathsf{p}\circ\mathsf{q}^* + \mathsf{q}\circ\mathsf{p}^*) = pq + \langle\mathbf{p},\mathbf{q}\rangle$, such that $|\mathsf{q}| = \sqrt{\mathsf{q}^*\circ\mathsf{q}} = \sqrt{q^2+\mathbf{q}^2}$ yields the modulus of a quaternion. All non-zero quaternions have a unique inverse $\mathsf{q}^{-1} = \mathsf{q}^*/|\mathsf{q}|^2$, such that $\mathsf{q}\circ\mathsf{q}^{-1} = \mathsf{q}^{-1}\circ\mathsf{q} = 1$ holds. Quaternions $\mathsf{q} = \mathbf{q}$ with a scalar part $\Re(\mathsf{q}) = 0$ are called *pure* (or *vector*) quaternions and identified with vectors in $\mathbb{E}^3$. The scalar and cross products of vector quaternions in $\mathbb{E}^3$ may be written as $\langle\mathbf{p},\mathbf{q}\rangle = -\frac{1}{2}(\mathbf{p}\circ\mathbf{q}+\mathbf{q}\circ\mathbf{p})$, and $\mathbf{p}\times\mathbf{q} = \frac{1}{2}(\mathbf{p}\circ\mathbf{q}-\mathbf{q}\circ\mathbf{p})$, as $\mathbf{p}\circ\mathbf{q} = -\langle\mathbf{p},\mathbf{q}\rangle + \mathbf{p}\times\mathbf{q}$ holds.

Proper rotations $\mathsf{R}\in\mathsf{SO}(3)$ may be represented by *unimodular* (or *rotational*) quaternions $\hat{\mathsf{q}} = q+\mathbf{q}$, satisfying $|\hat{\mathsf{q}}|^2 = q^2+\mathbf{q}^2 = 1$ and located on the unit sphere $S^3 \subset \mathbb{E}^4$, by means of the *Euler map* $\hat{\mathsf{q}} \mapsto \mathsf{R} = \mathfrak{E}(\hat{\mathsf{q}})$ implicitely defined via its operation on vectors $\mathbf{v}\in\mathbb{E}^3 \simeq \Im\mathbb{H}$ as: $\mathfrak{E}(\hat{\mathsf{q}})\cdot\mathbf{v} = \hat{\mathsf{q}}\circ\mathbf{v}\circ\hat{\mathsf{q}}^*$. Thus, the pair $\pm\hat{\mathsf{q}}$ represents the same proper rotation $\mathsf{R}(\hat{\mathsf{q}}) = \mathsf{R}(-\hat{\mathsf{q}})$, consistent with the fact that $S^3 \simeq \mathsf{SU}(2)$ yields a double covering of $\mathsf{SO}(3)$. The definition of $\mathfrak{E}(\hat{\mathsf{q}})$ implies the formulas $\mathsf{R}(\hat{\mathsf{p}})\cdot\mathsf{R}(\hat{\mathsf{q}}) = \mathsf{R}(\hat{\mathsf{p}}\circ\hat{\mathsf{q}})$ for the composition of rotations and $\mathsf{R}(\hat{\mathsf{q}})^T = \mathsf{R}(\hat{\mathsf{q}}^*)$ for the inverse rotation, as $\mathsf{R}(1) = \mathsf{I}$ holds. For general quaternions $\mathsf{q} = q+\mathbf{q}\in\mathbb{H}$, an explicit invariant formula for the Euler map $\mathfrak{E}:\mathbb{H}\to\mathbb{R}^+_0\,\mathsf{SO}(3)$ is given by $\mathsf{q}\mapsto\mathfrak{E}(\mathsf{q}) := (q^2-\mathbf{q}^2)\mathsf{I} + 2\mathbf{q}\otimes\mathbf{q} + 2q\tilde{\mathbf{q}} = |\mathsf{q}|^2\mathfrak{E}(\hat{\mathsf{q}})$, where $\hat{\mathsf{q}} := \mathsf{q}/|\mathsf{q}| \in S^3$. According to Euler, each proper rotation may be represented as $\mathsf{R} = \exp(\vartheta\,\tilde{\mathbf{u}})$, i.e.: a rotation by an angle ϑ around an axis determined by the unit vector $\hat{\mathbf{u}}$, with uniquely determined $\vartheta\in(0,2\pi)$ and $\hat{\mathbf{u}}\in S^2$ for $\mathsf{R}\neq\mathsf{I}$. The corresponding rotational quaternion is given by $\hat{\mathsf{q}} = \exp(\vartheta/2\,\hat{\mathbf{u}}) = \cos(\vartheta/2) + \sin(\vartheta/2)\,\hat{\mathbf{u}}$, such that $\mathfrak{E}(\pm\exp(\vartheta/2\,\hat{\mathbf{u}})) = \exp(\vartheta\,\tilde{\mathbf{u}}) = \cos(\vartheta)\mathsf{I} + \sin(\vartheta)\tilde{\mathbf{u}} + [1-\cos(\vartheta)]\,\hat{\mathbf{u}}\otimes\hat{\mathbf{u}}$ (with $\tilde{\mathbf{u}}^2 \equiv \hat{\mathbf{u}}\otimes\hat{\mathbf{u}} - \mathsf{I}$) holds identically.

Geometric curves in Euclidian space Here we collect some basics of curves in Euclidian space, as presented in standard texts like e.g. do Carmo's book [20] (see also Blaschke's books [9, 10]). We regard *geometric curves* as *simple arcs* [40] corresponding to smooth, one–dimensional connected submanifolds[8]. Thus, the mapping $\mathscr{C}\ni p\mapsto\xi(p)\in\mathbb{R}$ of the points p on a geometric curve $\mathscr{C}\subset\mathscr{E}^3$ to their real *coordinates* ξ is (at least once) differentiable and invertible, and the inverse mapping $\xi\mapsto p(\xi)$ from open intervals in $\mathbb{R}$ into $\mathscr{E}^3$ provides a local *parametrization* of the curve. By joining the open intervals of local parametrizations, we obtain a larger one $(a,b)\subset\mathbb{R}$ corresponding to a global parametrization $\phi:[a,b]\to\mathscr{C}$ of the geometric curve, such that $(a,b)\ni\xi\mapsto p=\phi(\xi)$ yields all interior points of $\mathscr{C}$, and the two boundary points of $\mathscr{C}$ are given by $\phi(a)$ and $\phi(b)$. The position vectors $\mathbf{x}(p)\in\mathbb{E}^3$ of curve points are then given by a *parameter curve* $\xi\mapsto\mathbf{r}(\xi) := \mathbf{x}(\phi(\xi))$ in $\mathbb{E}^3$.

The derivative of vector fields on a geometric curve For a vector field $\mathscr{C}\ni p\mapsto\mathbf{v}(p)\in\mathbb{E}^3$ mapping points on a smooth geometric curve to vectors in Euclician space, the derivative $\mathsf{d}\mathbf{v}_p : T_p\mathscr{C}\to T_{\mathbf{v}(p)}\mathbb{E}^3 \simeq \mathbb{E}^3$ is a linear mapping of tangent vectors (see [31] §1, or [4], Ch. 5 §34 sec. 4). For the tangent vectors $\mathbf{r}'(\xi) = \|\mathbf{r}'(\xi)\|\,\mathbf{t}(p(\xi))$ of the parameter curve $\mathbf{r}(\xi) = \mathbf{x}(p(\xi))$ induced by a (local) parametrization $\xi\mapsto p(\xi)$ of the curve and, by the usual abuse of notation, $\mathbf{v}(\xi)\equiv\mathbf{v}(p(\xi))$, the identities $\mathsf{d}\mathbf{v}_p(\mathbf{r}'(\xi)) = \|\mathbf{r}'(\xi)\|\mathsf{d}\mathbf{v}_p(\mathbf{t}(p(\xi))) = \mathbf{v}'(\xi)$ define the operation of $\mathsf{d}\mathbf{v}_p$ on tangent vectors. In particular, $\mathsf{d}\mathbf{v}_p(\mathbf{t}(p)) = \mathbf{v}'(s)$ for arc length parametrization, and $\mathsf{d}\mathbf{x}_p(\mathbf{t}(p))\equiv\mathbf{t}(p)$.

For $\mathbf{v}(p)\in S^2$ the derivative $\mathsf{d}\mathbf{v}_p : T_p\mathscr{C}\to T_{\mathbf{v}(p)}S^2$ maps tangent vectors to the tangent plane $T_{\mathbf{v}(p)}S^2$ to S^2 orthogonal to $\mathbf{v}(p)$, such that $\langle\mathbf{v}(p),\mathsf{d}\mathbf{v}_p(\mathbf{t}(p))\rangle = 0$ holds. This explains briefly the geometric meaning[9] of the derivative $\mathsf{d}\mathbf{a}^{(k)}_p$ of the directors of a moving frame $\mathsf{R}(p) = \mathbf{a}^{(k)}(p)\otimes\mathbf{e}_k$ on a geometric curve, as well as the derivative $\mathsf{d}\mathsf{R}_p$ of a moving frame field $\mathscr{C}\ni p\mapsto\mathsf{R}(p)\in\mathsf{SO}(3)$, and the derivative $\mathsf{d}\hat{\mathsf{q}}_p$ of a rotational quaternion field $\mathscr{C}\ni p\mapsto\hat{\mathsf{q}}(p)\in S^3\subset\mathbb{H}$ on $\mathscr{C}$. If $\mathsf{R}(p) = \mathfrak{E}(\hat{\mathsf{q}}(p))$, then the derivatives of the $\mathsf{SO}(3)$ frame and the rotational quaternion are related by $\mathsf{d}\mathsf{R}_p = \nabla_{S^3}\mathfrak{E}(\hat{\mathsf{q}}(p))\cdot\mathsf{d}\hat{\mathsf{q}}_p$ via the (tangential) gradient $\nabla_{S^3}\mathfrak{E}$ of the Euler map on S^3.

[7] It is always clear from the context whether a term $q+\mathbf{q}$ refers to the addition of the real and imaginary parts of a quaternion or the parallel displacement of a point in $\mathscr{E}^3$ by a vector.

[8] One–dimensional connected (sub)manifolds are either *simple arcs* diffeomorphic to an interval, or *simple loops* diffeomorphic to a circle (see the appendix of Milnor's booklet [31] for a proof).

[9] We refer to [10, 15, 39] for a systematic treatment of Cartan's derivative within the framework of differential forms and moving frames.

B Elastic energy of a Cosserat rod

The theory of *Continuum Mechanics of solid bodies* [23] provides proper physical models to simulate deformations of flexible parts. A continuum–mechanical model of a material body consists of three main constituents: *kinematics*, *equilibrium equations* and *constitutive laws*. Summarized briefly, the general programme of continuum mechanics aims at determining *equilibrium configurations* of a body subject to certain *boundary conditions*, such that all external *forces* acting on the body are *in equilibrium* with the internal ones (resulting from deformations of its shape) and inertial effects, making use of *constitutive laws* that relate local changes of shape, measured in terms of *strains*, to *stresses* that encode information on the corresponding local forces.

In continuum mechanics, one studies *deformations* of a material body, which are defined as a diffeomorphic (i.e.: bijective and differentiable) mappings $\Phi : \mathscr{B}_0 \to \mathscr{B}$ of a reference configuration $\mathscr{B}_0$ of the body to arbitrary configurations $\mathscr{B} = \Phi(\mathscr{B}_0)$. *Rigid* transformations leave the shape of the reference configuration undeformed. More precisely: the Euclidean distance $|p-q| = \|\mathbf{x}(p) - \mathbf{x}(q)\|$ of any pair $(p,q) \in \mathscr{B}$ of points remains identically the same as in the reference configuration. This implies that any rigid transformation is a combination of a translation and rotation in Euclidean space. The Lie group $\mathsf{SE}(3) = \mathbb{E}^3 \rtimes \mathsf{SE}(3)$ consists of the family of orientation preserving rigid transformations, equipped with the group operation of the semidirect product resulting from factoring out the normal subgroup of translations.

Static equilibria of deformed elastic structures can be computed as minima of their elastic energy, subject to the assumed boundary conditions. As we intend to model slender flexible structures as elastic Cosserat rods, we need to specify a corresponding elastic energy function. For linear elastic material behaviour, the elastic (*stored*) energy function of a 3D body is a quadratic form of its Green–Lagrange strain tensor $\mathsf{E} = \frac{1}{2}(\mathsf{F}^T \cdot \mathsf{F} - \mathsf{I})$, where $\mathsf{F} = \mathsf{d}\Phi(\mathbf{X})$ is the deformation gradient computed as the derivative of the positions $\mathbf{x} = \Phi(\mathbf{X})$ of the material points in the deformed body volume w.r.t. their postions $\mathbf{X}$ in the undeformed body (see [23] for details).

If one computes the deformation gradient and Green–Lagrange strain tensors for the deformed configurations $\mathbf{x} = \mathbf{r}(s) + \xi_\alpha \, \mathbf{a}^{(\alpha)}(s)$ of a Cosserat rod w.r.t. its undeformed reference configuration $\mathbf{X} = \mathbf{r}_0(s) + \xi_\alpha \, \mathbf{a}_0^{(\alpha)}(s)$ given by a smooth regular curve $\mathbf{r}_0(s)$ parametrized by arc length and its adapted frame $\mathsf{R}_0(s) = \mathbf{a}_0^{(k)}(s) \otimes \mathbf{e}_k$ with $\mathbf{r}_0'(s) = \mathbf{a}_0^{(3)}(s)$, one obtains [29] an exact closed form expression for E which depends on the differences $\mathbf{K}(s) - \mathbf{K}_0(s)$ and $\mathbf{\Gamma}(s) - \mathbf{\Gamma}_0$ (with $\mathbf{\Gamma}_0 = (0,0,1)^T$) of the invariants of the framed curve in their deformed and undeformed configurations.

For slender rod geometries, one may always assume that the local strains remain small, although the deformations of the rod configuration correspond to large (*finite*) rotations and displacements in space. In this case one may approximate the exact expression for E by taking only the leading order terms in the differences of the invariants into account. The resulting approximated energy density can then be integrated analytically over the cross section coordinates (ξ_1, ξ_2) in closed form, which finally yields [29] the elastic energy $\mathscr{W}_{el}$ of a Cosserat rod as a quadratic functional in the differences $\mathbf{K} - \mathbf{K}_0$ and $\mathbf{\Gamma} - \mathbf{\Gamma}_0$ of the invariants, given by the sum $\mathscr{W}_{el} = \mathscr{W}_{es} + \mathscr{W}_{bt}$ of the two integrals

$$\mathscr{W}_{es} = \frac{1}{2} \int_0^L ds \, [EA] \left(\Gamma^{(3)}(s) - 1 \right)^2 + [GA_\alpha] \Gamma^{(\alpha)}(s)^2 \,, \tag{20}$$

$$\mathscr{W}_{bt} = \frac{1}{2} \int_0^L ds \, [EI_\alpha] \left(K^{(\alpha)}(s) - K_0^{(\alpha)}(s) \right)^2 + [GJ] \left(K^{(3)}(s) - K_0^{(3)}(s) \right)^2 . \tag{21}$$

The first term (20) represents the elastic energy related to rod deformations by longitudinal *extension* combined with transverse *shearing*, the second term (21) accounts for the elastic energy stored in *bending* and *torsional* deformations of the rod.

The parameters $[EA], [GA_\alpha], [EI_\alpha]$ and $[GJ]$ quantify the *effective stiffness properties* of the local cross section of the rod related to the respective deformation mode. They may be constants, or vary along the rod as functions of s. In the simple case of a homogeneous and isotropic material characterized by the elastic moduli E and G, they are given as products of the moduli and geometric quantities (i.e.: area A, area moments I_α, polar moment J) of the cross section.

C Discrete elastic energy of quaternionic Cosserat rods

To discretize the energy integrals (20) and (21) we need a discrete model of framed curves with discrete versions of their invariants $\mathbf{K}$ and $\mathbf{\Gamma}$. We discretize the continuum model of an elastic Cosserat rod by approximating its elastic energy integrals (20) and (21) by suitable quadrature rules, making use of the discrete curvatures $\{K_j^{(k)}\}_{j=1,\dots,n-1}^{k=1,2,3}$ and extensional and shearing strains $\{\Gamma_{j-1/2}^{(k)}\}_{j=1,\dots,n}^{k=1,2,3}$. Here we briefly outline this approach described in detail in our article in [25].

We start with a discretization $0=:s_0<s_1<\ldots<s_n:=L$ of the interval domain $[0,L]$ of the arc length parameter s of the reference curve $\mathbf{r}_0(s)$ into subintervals $[s_{j-1},s_j]$ of length $h_{j-1/2}:=s_j-s_{j-1}$. The distance between interval midpoints $s_{j\pm1/2}=\frac{1}{2}(s_j+s_{j\pm1})$ is given by $\Delta s_j:=s_{j+1/2}-s_{j-1/2}=\bar{h}_j$, where $\bar{h}_j:=\frac{1}{2}(h_{j-1/2}+h_{j+1/2})$ is the average of the grid constants $h_{j\pm1/2}$ adjacent to s_j.

Discrete extensional and shear energy As the discrete extensional and shear strains $\Gamma_{j-1/2}^{(k)}$ are edge based quantities, an approximation of the energy integral (20) by midpoint quadrature is the natural choice to obtain a discrete version of $\mathscr{W}_{es}$. The pull back of the strains to the reference configuration is obtained by a rescaling with the factors $\ell_{j-1/2}/h_{j-1/2}\approx\|\mathbf{r}'(s_{j-1/2})\|$, according to

$$\bar{\Gamma}_{j-1/2}^{(k)} \;:=\; \frac{\ell_{j-1/2}}{h_{j-1/2}}\,\Gamma_{j-1/2}^{(k)} \;=\; \langle \mathbf{l}_{j-1/2}, \mathbf{a}_{j-1/2}^{(k)}\rangle/h_{j-1/2} \;=\; \langle \bar{\mathbf{\Gamma}}_{j-1/2}, \mathbf{e}_k\rangle\,, \tag{22}$$

where $\bar{\mathbf{\Gamma}}_{j-1/2}:=\hat{\mathsf{q}}_{j-1/2}^{*}\circ(\mathbf{l}_{j-1/2}/h_{j-1/2})\circ\hat{\mathsf{q}}_{j-1/2}$ is the material vector obtained from rotating the discrete edge tangent vector $\mathbf{l}_{j-1/2}/h_{j-1/2}$ back to the local frame. The discrete approximation of $\mathscr{W}_{es}$ can be written in compact form as

$$\mathscr{W}_{es} \;\approx\; \mathscr{W}_{es}^{(D)} \;:=\; \frac{1}{2}\sum_{j=1}^{n} h_{j-1/2}\,\langle \Delta\bar{\mathbf{\Gamma}}_{j-1/2}, \mathsf{C}_{es}\cdot\Delta\bar{\mathbf{\Gamma}}_{j-1/2}\rangle\,, \tag{23}$$

where $\Delta\bar{\mathbf{\Gamma}}_{j-1/2}:=\bar{\mathbf{\Gamma}}_{j-1/2}-\mathbf{\Gamma}_0$ with $\mathbf{\Gamma}_0=(0,0,1)^T$, and the shear and extensional stiffness parameters collected in the diagonal matrix $\mathsf{C}_{es}:=\mathrm{diag}([GA_1],[GA_2],[EA])$.

The condition of vanishing discrete transverse shear strains $\bar{\Gamma}_{j-1/2}^{(\alpha)}\equiv 0$ implies $\bar{\Gamma}_{j-1/2}^{(3)}=\ell_{j-1/2}/h_{j-1/2}$, such that (22) reduces to the extensional energy

$$\mathscr{W}_{ext}^{(D)} \;:=\; \frac{1}{2}\sum_{j=1}^{n} h_{j-1/2}\,[EA]\,\left(\ell_{j-1/2}/h_{j-1/2}-1\right)^2$$

of a *discrete extensible Kirchhoff rod* model [28], which approximates its continuum counterpart given by the functional $\mathscr{W}_{ext}:=\frac{1}{2}\int_0^L ds\,[EA]\,(\|\mathbf{r}'(s)\|-1)^2$ of the centerline. Additionally imposing the *inextensibility condition* $\ell_{j-1/2}\equiv h_{j-1/2}$ on the edges implies $\mathscr{W}_{ext}^{(D)}\equiv 0\equiv\mathscr{W}_{es}^{(D)}$.

Discrete bending and torsion energy The discrete curvatures $K_j^{(k)}$ are vertex based quantities, such that a discrete approximation of $\mathscr{W}_{es}$ can be obtained from the energy integral (21) by (non-equidistant) trapezoidal quadrature. The pull back of the curvatures originally defined w.r.t. discrete arc length to the reference configuration implies a rescaling by the factor $\Delta\varsigma_j/\Delta s_j\approx\|\mathbf{r}'(s_j)\|$, i.e.: $\bar{K}_j^{(k)}:=(\Delta\varsigma_j/\Delta s_j)\,K_j^{(k)}$, equivalent to the definition

$$\bar{K}_j^{(k)} \;:=\; \langle \bar{\mathbf{K}}_j, \mathbf{e}_k\rangle\,,\;\; \bar{\mathbf{K}}_j \;:=\; (\Delta s_j)^{-1}\,2\log\hat{\mathsf{W}}_j \;=\; (\vartheta_j/\Delta s_j)\,\hat{\mathbf{U}}_j \;=\; \bar{K}_j^{(k)}\,\mathbf{e}_k \tag{24}$$

of discrete pulled back material curvatures. The discrete approximation of $\mathscr{W}_{bt}$ can then be written in compactly as

$$\mathscr{W}_{bt} \;\approx\; \mathscr{W}_{bt}^{(D)} \;:=\; \frac{1}{2}\sum_{j=0}^{n} \Delta s_j\,\langle \Delta\bar{\mathbf{K}}_j, \mathsf{C}_{bt}\cdot\Delta\bar{\mathbf{K}}_j\rangle\,, \tag{25}$$

with the curvature differences $\Delta\bar{\mathbf{K}}_j:=\bar{\mathbf{K}}_j-\mathbf{K}_{\mathbf{0}\,j}$ between the deformed and reference configurations, the diagonal matrix $\mathsf{C}_{bt}:=\mathrm{diag}([EI_1],[EI_2],[GJ])$ of bending and torsional stiffness parameters, and the grid constants of the half–edges near the boundary defined as $\Delta s_0:=h_{1/2}/2$ and $\Delta s_n:=h_{n-1/2}/2$.

Boundary conditions The definition of material curvature vectors $\bar{\mathbf{K}}_0$ and $\bar{\mathbf{K}}_n$ at the boundary vertices is a new element in the discrete model that did not have to be considered in the theory of discrete Cosserat curves up to this point. These discrete curvatures are defined in the deformed configuration in terms of the material difference rotations $\hat{\mathsf{W}}_0 := \hat{\mathsf{q}}_0^* \circ \hat{\mathsf{q}}_{1/2}$ and $\hat{\mathsf{W}}_n := \hat{\mathsf{q}}_{n-1/2}^* \circ \hat{\mathsf{q}}_n$ connecting the *boundary frames* $\hat{\mathsf{q}}_0$ and $\hat{\mathsf{q}}_n$ to the frames on the adjacent edges, with analogous definitions for the boundary curvatures of the reference configuration.

The boundary frames of both configurations are determined by *boundary conditions* imposed on the discrete rod model, which have to be formulated as separate conditions, or can directly be built into the discrete energy $\mathscr{W}_{bt}^{(D)}$. Likewise, boundary conditions on the vertices p_0 and p_n influence the discrete energy $\mathscr{W}_{es}^{(D)}$.

Discrete equilibrium equations With the boundary conditions built into the respective terms of the discrete energies (23) and (25), the total discrete elastic energy given by

$$\mathscr{W}_{el}^{(D)}(\mathscr{X}_f) \;:=\; \mathscr{W}_{es}^{(D)}(\mathscr{X}_f) \;+\; \mathscr{W}_{bt}^{(D)}(\mathscr{X}_f) \tag{26}$$

become functions of the free vertex positions $\{\mathbf{r}_j\}$ and quaternion frames $\{\hat{\mathsf{q}}_{j-1/2}\}$ collected in the set $\mathscr{X}_f := \{\mathbf{r}_j\} \cup \{\hat{\mathsf{q}}_{j-1/2}\}$ of free variables.

Static equilibirum configurations of a discrete Cosserat rod subject to given boundary conditions can be obtained by *minimizing the discrete elastic energy* of the rod. The *discrete equilibrium equations*

$$\nabla_{\mathscr{X}_f} \mathscr{W}_{el}^{(D)}(\mathscr{X}_f) \;=\; 0 \;\Leftrightarrow\; \frac{\partial \mathscr{W}_{el}^{(D)}}{\partial \mathbf{r}_j}(\mathscr{X}_f) \;=\; \mathbf{0}\;,\; \frac{\partial \mathscr{W}_{el}^{(D)}}{\partial \hat{\mathsf{q}}_{j-1/2}}(\mathscr{X}_f) \;=\; \mathbf{0} \tag{27}$$

provide a necessary condition for such energy minima. The discrete equilibrium equations (26) is a coupled nonlinear system of algebraic equation, which can be solved numerically by Newton's method. Alternatively, one can find approximate equilibrium configurations by energy minimization, using nonlinear conjugate gradients or Quasi-Newton type optimization methods like BFGS.

The system (26) is actually a special case of the dynamic equilibrium equations for a semi–discrete model of time dependent discrete quaternionic Cosserat rods [25] given by the Euler–Lagrange equations

$$\partial_t \left(\nabla_{\partial_t \mathscr{X}_f} \mathscr{L}^{(D)}(\mathscr{X}_f, \partial_t \mathscr{X}_f) \right) \;-\; \nabla_{\mathscr{X}_f} \mathscr{L}^{(D)}(\mathscr{X}_f, \partial_t \mathscr{X}_f) \;=\; 0$$

for the Lagrangian function $\mathscr{L}^{(D)}(\mathscr{X}_f, \partial_t \mathscr{X}_f) := \mathscr{T}_{kin}^{(D)}(\mathscr{X}_f, \partial_t \mathscr{X}_f) - \mathscr{W}_{el}^{(D)}(\mathscr{X}_f)$ defined as the difference of the kinetic and potential energy according to the general concepts of Lagrangian mechanics (see [25, 26] for details).

The benefits of a discretization by geometric finite differences The various steps to obtain a discrete energy function from a continuum functional and the approach to compute static or dynamic equilibrium configurations as solutions of the Euler–Lagrange equations did not involve any specific aspects of the discrete geometry of the underlying model so far. The essential ingredient to this procedure is provided by the fact that the curvatures and strains are well defined for arbitrarily large deformations, independent of the coarseness of the discretization, as the discrete curvatures increase with increasing values of the angles, up to their limit values corresponding to degenerate configurations, such that the elastic energy vanishes exactly only in the reference configuration and does not possess[10] any "artificial" minima otherwise. This points out how our approach to construct a discrete theory of framed curves by *geometric finite differences* results in a rod model that behaves qualitatively correct even for very coarse discretizations. In this sense, one can state that our discrete Cosserat rod model inherits its structural stability and its qualitatively correct physical behaviour at arbitrarily coarse discretizations from our underlying kinematic model of discrete Cosserat curves.

[10]Note that not all discretization schemes share these important properties, e.g.: A finite element approach using linear interpolation of nodal $\mathsf{SO}(3)$ frames yields discrete curvatures $\sim \sin(\vartheta_j)\,\hat{\mathbf{u}}_j$ (see the discussion in Remark 8 of [24]), which becomes extremal at $\vartheta_j = \pm\pi/2$ and then decreases in modulus for larger values of ϑ_j, up to the value zero taken in the degenerate case $\vartheta_j = \pm\pi$. For coarse discretizations, it can easily happen that bending or torsion angles $|\vartheta_j| \approx \pi/2$ occur. A model based on this discretization of curvature would obviously produce unphysical results, as zig-zag type configurations with angles $\pi/2 \leq |\vartheta_j| \leq \pi$ become energetically favourable.

References

[1] Antman, S.S.: Kirchhoffs problem for nonlinearly elastic rods, *Quart. Appl. Math.* **32**, pp. 221-240 (1974).

[2] Antman, S.S.: *Nonlinear Problems of Elasticity*, Springer (2005).

[3] Arnol'd, V.I.: *Mathematical Methods of Classical Mechanics (2^{nd} ed.)*, Springer (1989).

[4] Arnol'd, V.I.: *Ordinary Differential Equations (1^{st} ed.)*, Springer (1992).

[5] Berdichevsky, V.L.: On the energy of an elastic rod, *J. Appl. Math. Mech. (PMM)* **45**(4), pp. 518–529 (1981).

[6] Berdichevsky, V.L.: *Variational Principles of Continuum Mechanics, Vol. I: Fundamentals, Vol. II: Applications*, Springer (2009).

[7] Bergou, M., Wardetzky, M., Robinson, S., Audoly, B., Grinspun, E.: Discrete Elastic Rods, *ACM Transaction on Graphics (SIGGRAPH)*, Vol. **27**(3), pp. 63:1–63:12 (2008).

[8] Bishop, R.L.: There is more than one way to frame a curve, *The American Mathematical Monthly* **82**(3), pp. 246–251 (1975).

[9] Blaschke, W.: *Vorlesungen über Differentialgeometrie. I. Elementare Differentialgeometrie (3. Aufl.)*, Springer, Berlin (1930).

[10] Blaschke, W., Reichardt, H.: *Einführung in die Differentialgeometrie*, Springer (1960).

[11] Bobenko, A.I., Suris, Yu.B.: Discrete time Lagrangian mechanics on Lie groups, with an application on the Lagrange top, *Comm. Math. Phys.* **204**, pp. 147–188 (1999).

[12] Bobenko, A.I., Schröder, P., Sullivan, J.M., Ziegler, G.M. (Eds.): *Discrete Differential Geometry*, Series: Oberwolfach Seminars, Vol. 38, Birkhäuser (2008).

[13] Borri, M. and Bottasso, C.: An intrinsic beam model based on a helicoidal approximation – Part I: Formulation, *Int. J. Numer. Methods Eng.*, Vol. **37**(13), pp. 2267–2289 (1994).

[14] Cardona, A. and Geradin, M.: A beam finite element non-linear theory with finite rotations, *Int. J. Numer. Methods Eng.*, Vol. **26**(11), pp. 2403–2438 (1988).

[15] Cartan, H.: *Formes différentielles — Applications élémentaires au calcul des variations et à la théorie des courbes et des surfaces*, Hermann, Paris (1967).

[16] Chouaieb, N. and Maddocks, J.H.: Kirchhoff's Problem of Helical Equilibria of Uniform Rods, *Journal of Elasticity* **77**, pp. 221–247 (2000).

[17] Chouaieb, N., Goriely, A. and Maddocks, J.H.: Helices, *Proc. Nat. Acad. Sci.* **103**(25), pp. 9398-9403 (2006).

[18] Češarek, P., Saje, M. and Zupan, D.: Kinematically exact curved and twisted strain-based beam, *Int. J. Sol. Struct.*, Vol. **49**(13), pp. 1802–1817 (2012).

[19] Crisfield, M.A. and Jelenić, G.: Objectivity of strain measures in the geometrically exact three-dimensional beam theory and its finite-element implementation, *Proc. Royal Soc. London A: Math. Phys. Eng. Sciences*, Vol. **455**(1983), pp. 1125–1147 (1999).

[20] do Carmo, M.P.: *Differential Geometry of Curves and Surfaces*, Prentice–Hall (1976).

[21] Ebbinghaus, H.-D., Hermes, H., Hirzebruch, F., Koecher, M., Mainzer, K., Neukirch, J., Prestel, A., Remmert, R.: *Numbers*, Springer (1991).

[22] Géradin, M., Cardona, A.: *Flexible Multibody Dynamics: A Finite Element Approach*, John Wiley & Sons (2001).

[23] Gurtin, M.E.: *An Introduction to Continuum Mechanics*, Academic Press (1981).

[24] Jung, P., Leyendecker, S., Linn, J., Ortiz, M.: A discrete mechanics approach to the Cosserat rod theory - Part 1: static equilibria, *Int. J. Numer. Methods Eng.*, Vol. **85**(1), pp. 31–60 (2011).

[25] Lang, H., Linn, J., Arnold, M.: Multibody dynamics simulation of geometrically exact Cosserat Rods, *Multibody System Dynamics*, Vol. **25**(3), pp. 285–312 (2011).

[26] Lang, H., Arnold, M.: Numerical aspects in the dynamic simulation of geometrically exact rods, *Applied Numerical Mathematics*, Vol. **62**, pp. 1411–1427 (2012).

[27] Linn, J. and Dreßler, K.: Discrete Cosserat rod models based on the difference geometry of framed curves for interactive simulation of flexible cables, 29 p., to be published in L. Ghezzi, D. Hömberg and C. Landry (Eds.): *Math for the Digital Factory*, Springer (2016).

[28] Linn, J., Stephan, T., Carlsson, J., Bohlin, R.: Fast Simulation of Quasistatic Rod Deformations for VR Applications. L.L. Bonilla, M. Moscoso, G. Platero and J.M. Vega (Eds.): *Progress in Industrial Mathematics at ECMI 2006*, pp. 247–253, Springer (2008).

[29] Linn, J., Lang, H., Tuganov, A.: Geometrically exact Cosserat rods with Kelvin–Voigt type viscous damping, Mechanical Sciences, Vol. **4**, pp. 79–96, 2013.

[30] Love, A.E.H.: *A Treatise on the Mathematical Theory of Elasticity (*4^{th} *edition)*, Cambridge University Press (1927)

[31] Milnor, J.W.: *Topology from the Differentiable Viewpoint*, The University Press of Virginia (1965); reprint: Princeton University Press (1997).

[32] Reissner, E.: On one-dimensional large-displacement finite-strain beam theory, *Stud. Appl. Math.* **52**, pp. 87–95 (1973).

[33] Sander, O.: Geodesic finite elements for Cosserat rods, *Int. J. Numer. Methods Eng.*, Vol. **82**(1), pp. 1645-1670 (2010).

[34] Sauer, R.: *Differenzengeometrie*, Springer (1970).

[35] Shoemake, K.: Animating rotation with quaternion curves, *ACM SIGGRAPH Computer Graphics*, **19** (3), pp. 245–254 (1985).

[36] Simo, J.C.: A finite strain beam formulation: the three dimensional dynamic problem – Part I, *Comput. Meth. Appl. Mech. Eng.*, Vol. **49**(1), pp. 55–70 (1985).

[37] V. Sonneville, A. Cardona, and O. Brüls: Geometrically exact beam finite element formulated on the special Euclidean group $SE(3)$, *Comput. Meth. Appl. Mech. Eng.*, Vol. **268**, pp. 451–474 (2014).

[38] V. Sonneville, A. Cardona, and O. Brüls: Geometric interpretation of a non–linear beam finite element on the Lie group $SE(3)$, *Ar. Mech. Eng.*, Vol. **61**(2), pp. 305–329 (2014).

[39] Sternberg, S.: *Curvature in Mathematics and Physics*, Dover (2012).

[40] Sullivan, J.M.: Curves of finite total curvature (pp. 137–161), Curvatures of smooth and discrete surfaces (pp. 175–188), in [12], Part II: *Curvatures of Discrete Curves and Surfaces*.

[41] Wriggers, P.: *Nonlinear Finite Elements*, Springer (2008).